Organic carbon source variability in Arctic bivalves as deduced from the compound specific carbon isotopic composition of amino acids

Monika Kędra[a,*], Lee W. Cooper[b], Marc J. Silberberger[a], Mengjie Zhang[b], Dana Biasatti[b,c], Jacqueline M. Grebmeier[b]

[a]Institute of Oceanology Polish Academy of Sciences, Powstańców Warszawy 55 81-712 Sopot Poland

[b]University of Maryland Center for Environmental Sciences, Chesapeake Biological Laboratory, Solomons, MD, 20688 United States

[c]University of Notre Dame, Center for Environmental Science and Technology, Notre Dame, IN, 46556 United States (present address)

* Corresponding author: Tel: (+48 58) 73 11 779; Fax: (+48 58) 551 21 30

E-mail address: kedra@iopan.gda.pl (M. Kędra)

The authors declare that they have no known competing financial interests or personal relationships that could have appeared to influence the work reported in this paper.

Authors contributions: MK - sample collection (DBO), data analysis, ms writing, funding (Polish National Science Centre), LC - sample collection, ms editing, funding (US NSF, BOEM), MS - data analysis (model), ms editing, MZ - sample collection (HS), sample analysis (CSIA-AA), DB - sample analysis (CSIA-AA), ms editing, JG - sample collection, ms editing, funding (US NSF, BOEM).

Abstract

In this study we used compound-specific carbon isotope analysis of amino acids ($\delta^{13}C_{AA}$) to determine organic carbon sources utilized by the dominant benthic bivalve species collected along a latitudinal gradient in the northern Bering and Chukchi Seas, specifically at productivity hotspots identified within the Distributed Biological Observatory (DBO) program, and over Hanna Shoal in the northern Chukchi Sea. The recent shift to earlier sea-ice melt is one of the climate change consequences influencing Pacific Arctic ecosystems, which we integrate within our observations. Our goals included investigating the utilization of organic matter (OM) resources by several dominant Arctic bivalves and their trophic elasticity to changes in primary productivity patterns following changes in the onset of the annual productive season. Based upon $\delta^{13}C_{AA}$ patterns observed, these species utilized different carbon sources along the latitudinal gradient, including a strong input of bacterially reworked material and microalgae, mainly in particulate organic matter mixtures. Species type and the sampling location both played roles in $\delta^{13}C_{AA}$ variability, suggesting the influence of local production and decomposition processes. *Macoma calcarea* and *Ennucula tenuis* were shown to utilize organic matter of different quality, suggesting they may switch their feeding preferences to more detrital sources on a seasonal basis, but this was also affected by geographical location. These observations may have important implications for the benthic populations as microbial reworking of organic material is expected to increase with climate warming and likely shifts in food web structure.

Key words: Food source, Pacific Arctic, Sea-ice retreat, Benthos, Stable isotopes, Amino acids, Fingerprinting

1. Introduction

Over the last several decades seasonal Arctic sea-ice cover has been decreasing at rates that are historically unprecedented (IPCC, 2019; Meier, 2017; Polyakov, et al., 2012). The sea-ice cover reduction is accompanied by a reduction in sea-ice thickness and a shift from multi-year to largely seasonal sea-ice cover (Comiso, 2012; Kwok and Rothrock, 2009; Parkinson and Comiso, 2013; Serreze and Meier, 2019). This trend is particularly prominent in the northern Bering and Chukchi Seas where rapid changes in seasonal sea-ice cover patterns and persistence are observed (Frey, et al., 2014, 2015, 2018; Walsh, et al., 2016; Grebmeier et al., 2018). Accelerating sea-ice cover reductions in this region are further amplified by increased heat fluxes into the Arctic Ocean through Bering Strait (Woodgate, et al., 2010; 2012; Woodgate, 2018) and summertime warming anomalies (Steele, et al., 2008; Timmermans and Proshutinsky, 2015; Timmermans, et al., 2018). This 'new normal' that is associated with an increase in seasonal seawater temperature introduces important concerns about its influence on ecological processes and potential cascading effects through food webs in the Pacific Arctic (Moore and Stabeno, 2015).

Changing seasonal sea-ice conditions and seawater temperatures strongly influence primary production (PP) regimes in the Arctic, and thus food webs, energy transfer through food webs and marine ecosystems (Grebmeier, 2012; Kędra, et al., 2015; Moran, et al., 2005). On shallow Arctic shelves, benthic communities are rich and diverse, and benthic food webs play an important role in overall system production, turnover rates and remineralization (Grebmeier; et al., 2015a; Iken, et al., 2010). Predicted changes in PP in shelf ecosystems will impact pelagic-benthic coupling processes, benthic food webs, and whole ecosystem functioning (Moran, et al., 2005; Grebmeier, et al., 2018). The extended phytoplankton growth season and sea-ice melt

result in increase in net PP of open water phytoplankton (Ardyna and Arrigo, 2020; Arrigo and van Dijken, 2011, 2015; Arrigo, et al., 2014; Assmy, et al., 2017; Mundy, et al., 2014) and decrease of sea-ice algae contribution to PP, both important potential food sources for benthic populations. Longer open water period result in more time for microbial and zooplankton processing of water column material. In Arctic sediments, organic matter (OM) from freshly deposited microalgae (phytoplankton and/or sea-ice algae) can be rapidly converted into bacterial biomass (Sun, et al., 2009) forming another potential food source for benthic organisms, in the form of degraded microalgae, microbe-derived OM, and/or the microbes themselves (Lovvorn, et al., 2005; McTigue and Dunton, 2014; McTigue, et al., 2015). Changes in timing and quality of the bloom, and therefore in the export fluxes of OM to the sea floor, and changes in the microbial reworking rate of this OM may affect benthic species composition, abundances and functioning (Ambrose and Renaud, 1997; Morata, et al., 2015; 2020). Trophic relationships in Arctic food webs have received significant scientific attention in the northern Bering (e.g. Lovvorn, et al., 2005; North, et al., 2014) and Chukchi seas (e.g. Feder, et al., 2011; Iken, et al., 2010; North, et al., 2014; Rowe, et al., 2019; Tu, et al., 2015). However, understanding trophic relationships in food webs with multiple organic carbon sources (e.g. sea-ice algae, phytoplankton, bacteria), where bacterially reworked OM is common (Kędra et al., 2019; Lovvorn, et al., 2005; North, et al., 2014), remains a continuing challenge in ecological studies.

Commonly used methods to assess marine food web structure in the Arctic involve the use of lipids and fatty acids, including compound specific $\delta^{13}C$ values (e.g. Koch, et al., 2020; Kohlbach, et al., 2019; McGovern, et al., 2018; Mohan, et al., 2016; Schollmeier, et al., 2018; Sun, et al., 2009), and the use of naturally occurring stable isotope ratios of nitrogen ($^{14}N/^{15}N$, expressed as $\delta^{15}N$) and carbon ($^{13}C/^{12}C$, expressed as $\delta^{13}C_{Bulk}$) to distinguish trophic

levels and food sources (e.g. Divine, et al., 2017; Feder, et al., 2011; Iken, et al., 2010, 2005; Kędra, et al., 2012). However, the combined effects of multiple sources and isotopic fractionation can make interpretation challenging (Post, 2002). In recent years, the growing use of gas chromatographic separation approaches that are linked to isotope ratio mass spectrometry has facilitated more rapid and efficient analysis of the stable isotope composition of amino acids (AAs). Naturally occurring $\delta^{13}C$ values of individual AAs ($\delta^{13}C_{AA}$) can be directly linked to the biosynthetic origin of material supporting animal food webs (Larsen, et al., 2009, 2013, 2015). Primary producers and bacteria can synthesize essential AAs *de novo*; however, most animals cannot synthesize essential AAs at a rate sufficient for adequate growth (Reeds, 2000), and therefore must incorporate them directly from their diet (McMahon, et al., 2010, 2016). Essential AAs (Lys – lysine, Phe – phenylalanine, Thr – threonine, Ile – isoleucine, Leu – leucine, Val – valine, Met – methionine) show negligible heavy isotope enrichment at each succeeding trophic level, and can act as 'fingerprints' of producer source in consumers (Larsen, et al., 2009). For example, Larsen, et al. (2012) showed that the relationships among the essential $\delta^{13}C_{AA}$ values can be used to differentiate between marine and terrestrial sources of OM and to estimate the contributions of various carbon sources to particulate organic matter (POM) and to detrital food webs. By comparison, for non-essential AAs (Gly – glycine, Ser – serine, Tyr – tyrosine, Ala – alanine, Asp – aspartic acid, Glu – glutamic acid, Pro – proline) the difference in $\delta^{13}C$ values for consumers relative to primary producers is highly variable (McMahon, et al., 2013). Taken together, the compound specific approach can therefore provide potentially additional insights over $\delta^{13}C_{Bulk}$ analysis of OM for PP source detection (Chikaraishi, et al., 2009, 2014; Larsen, et al., 2015, 2013, 2012; McClelland and Montoya, 2002; McMahon, et al., 2016, 2010; Nielsen, et al., 2015). This technique may be particularly useful in Arctic marine ecosystems, where OM available for organisms at the sea floor and in sediments contains a mixture of AAs derived from

120 variety of original autotrophic sources and those that have been subjected to diagenetic alteration
121 including heterotrophic bacterial degradation and/or *de novo* synthesis (McCarthy, et al., 2007).
122 The compound-specific isotope analyses of amino acids (CSIA-AA) methodology, and $\delta^{13}C_{AA}$
123 values in particular, has recently been applied in controlled feeding experiments on fish and
124 penguins (McMahon, et al., 2010, 2015; Rogers, et al., 2019), in laboratory cultures (Larsen, et
125 al., 2009, 2013, 2015), and in natural spatially and temporally variable environments with various
126 animals including turtles, penguins, reef and riverine fish, and Atlantic walruses (e.g. Arthur, et
127 al., 2014; Lorrain, et al., 2009; Sabadel, et al., 2016; 2020; Yurkowski, et al., 2020). Marine
128 benthic studies have been less prominent but have included work on corals, mussels and kelps
129 (Elliot Smith et al., 2018; McMahon, et al., 2016, 2018; Rowe et al., 2019; Schiff, et al., 2014;
130 Vokhshoori, et al., 2014).

131 The main objective of our study was to investigate the utilization of OM resources by
132 common bivalve species as focal species through use of CSIA-AA and $\delta^{13}C_{AA}$ patterns on the
133 Pacific Arctic shelf. Several studied bivalve species are dominant (in terms of biomass) among
134 benthic species in the region, but individually have different feeding behaviors. These bivalves
135 are also important food items for higher trophic level marine animals (e.g. spectacled eiders
136 (*Somateria fischeri*), Pacific walrus (*Odobenus rosmarus divergens*) and bearded seals
137 (*Erignathus barbatus*)), and their populations have been responding to changes in the OM
138 distribution patterns in recent years (e.g. Grebmeier, 2012; Grebmeier et al., 2015a; b; 2018).
139 Sampling station locations within the Distributed Biological Observatory (Moore and Grebmeier,
140 2018) were chosen to reflect possible differences in food sources along the latitudinal gradient.
141 We hypothesized that bivalves collected in July in the more northern areas, where sea-ice
142 persisted longer (i.e. the southern Chukchi Sea (DBO3), north-eastern Chukchi Sea (DBO4), in
143 Barrow Canyon (DBO5), and Hanna Shoal (HS)) would have a higher traceable ice algal isotopic

signature in their tissues than specimens collected in the northern Bering Sea where sea-ice retreats earlier in the year (i.e. south of the St. Lawrence Island (DBO1) and in the Chirikov Basin (DBO2)) (Fig. 1, 2). This variability is a consequence of the rapid deposition of sea ice-derived organic carbon after sea-ice break up (Ambrose, et al., 2001; Cooper, et al., 2005; Roca-Martí et al., 2016). This event occurs 6 to 8 weeks later at DBO4 and DBO5 compared to DBO1 (Grebmeier, et al., 2015a). Thus, in the Chukchi Sea, the more northern location, ice algal production is expected to be available to the benthos by June (DBO3) and June/July (DBO4, DBO5, HS). By comparison, ice algal production descends to the benthos in April/May in the more southern locations in the northern Bering Sea (DBO1 and DBO2) (Grebmeier and Cooper, 2016). Therefore, we hypothesized that the relative importance of microalgal (water column) derived AAs in the diet of the studied bivalves increases from south to north while the degree of bacterial reworking decreases northwards. This would reflect the time that had passed after the break-up of sea-ice and the annual peak flux of algae to the benthos at that time as well as the overall persistence of sea-ice free waters (Fig. 1, 2).

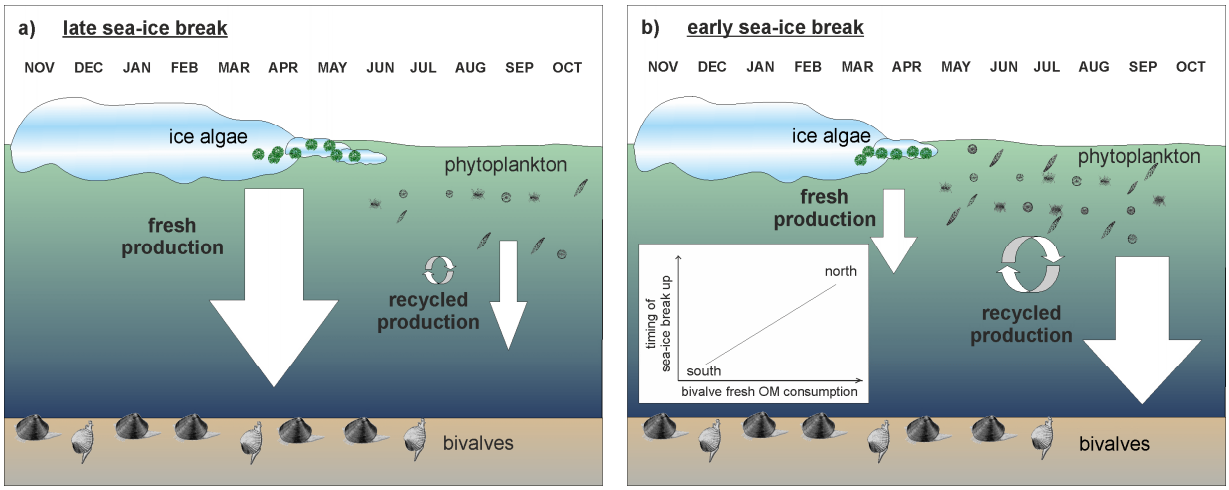

Fig. 1. Conceptual diagram showing two scenarios: a) when late sea-ice breakup occurs, fresh sea-ice production is exported to depth, with water column production only partly recycled in the

161 water column before reaching the benthos (northern areas of this study); and b) when sea-ice
162 breaks up earlier in the year, with less of the fresh production reaching the sea floor, more
163 recycled organic matter occurs in the open water period and descends to the benthos (southern
164 areas of this study). The insert shows the relation between bivalves' fresh organic matter
165 consumption and the timing of sea ice break-up.
166
167 2. Material and Methods
168
169 *2.1. Study area*
170
171 The northern Bering and Chukchi Seas are very productive shallow shelf systems
172 influenced by Pacific water masses (e.g. Grebmeier, et al., 2006), and are the focus of the DBO
173 that is documenting ecosystem responses to changing sea-ice cover, warmer water temperatures,
174 and other physical changes. The DBO was established as a change detection array for the
175 identification and consistent seasonal and interannual monitoring of biophysical responses to the
176 on-going climate related changes in the Pacific Arctic Region (Moore and Grebmeier, 2018).
177 Each DBO area was previously identified as biologically important with high levels of benthic
178 macrofaunal biomass and/or biodiversity, and these locations have been characterized as "hot
179 spots" with enhanced deposition of OM to the benthos (Grebmeier, 2012; Grebmeier, et al., 2010,
180 2015a, b).
181 The seasonal sea-ice cover in this region usually reaches a maximum in March and a
182 minimum in September and persists longer at higher latitudes (Grebmeier, et al., 2015a; Fig. 2).
183 However, recent climate warming affects sea-ice formation and persistence (Frey, et al., 2014.,
184 2015, 2018). An assessment of sea-ice trends from 1979 through 2014 in the Chukchi Sea

showed that sea-ice retreats to the northern shelf break (150 m contour) in summer occurred 0.7 days earlier per year (Serreze, et al., 2016). Extreme changes in ice pack thickness have occurred in September, with thinning equivalent to 51 cm decade^{-1} in the Chukchi Sea, leading to projections that the Pacific Arctic Region is moving towards an entirely first year ice pack (Frey, et al., 2014). Surface-intensified, nutrient-poor, warm and fresher (<31.8) Alaska Coastal Water flowing along the Alaskan coast, nutrient-rich and more saline (>32.5) Anadyr Water near the Siberian coast and moderately warm, intermediate saline (31.8–32.5) Bering Shelf Water are the main water masses in the region (Grebmeier, et al., 2006; Weingartner, et al., 2005; Woodgate, et al., 2005a, b). These water masses redistribute nutrients and algal production, organic carbon, and zooplankton from the Bering slope and the central Bering shelf into the northern Bering and Chukchi seas and thus strongly influence the intensity of local primary and secondary production (Grebmeier, et al., 2015a; Lowry, et al., 2015; Walsh, et al., 1989; Weingartner, et al., 2005; Woodgate, et al., 2012). PP is estimated to reach up to 570 g C m^{-2} yr^{-1} (Springer, et al., 1996) with higher values (maximum up to 840 g C m^{-2} yr^{-1}) in the southern Chukchi Sea (Springer and McRoy, 1993). However, over recent years a decline in PP has been reported in the northern Bering Sea (Lee, et al., 2012). In contrast, increases in PP have been observed in the Chukchi Sea southern coastal waters (Hirawake, et al., 2012; Petrenko, et al., 2013), including over Hanna Shoal, a shallow water feature, likely influenced by the earlier timing of sea-ice retreat (Hill, et al., 2018).

The total organic carbon (TOC) content in the surface sediments is high in deposition areas and is positively correlated with silt and clay content (Grebmeier and Cooper, 1995, 2014). Offshore sediments are dominated by muds and muddy sands, finer silts and clays occur on the slope while gravel, pebbles, rocks and sand dominate close to St. Lawrence Island, in nearshore regions of the Chirikov Basin, Bering Strait, and near the Alaskan coast (Fig. 2; Grebmeier and

209 Cooper, 2014; Grebmeier, et al., 2006; Pisareva, et al., 2015). Tight pelagic-benthic coupling
210 results in high benthic biomass (from 440±231 g wet weight m^{-2} in DBO1, the most southern
211 DBO transect, to 887±778 g wet weight m^{-2} in DBO3 (Grebmeier, et al., 2015a) and ~2800 g wet
212 weight m^{-2} in DBO5 (most northern DBO transect sampled; Grebmeier, et al., 2006). Each of the
213 DBO transect grids (see Fig. 2 for locations) are to different extents foraging areas for benthic
214 feeding marine mammals like gray whales or walruses, and sea birds such as spectacled eiders
215 (Grebmeier, 2012; Grebmeier and Barry, 2007; Grebmeier, et al., 2006; Sheffield and Grebmeier,
216 2009; Moore and Kuletz 2018).
217
218 *2.2. Sampling*
219
220 For sampling locations, we used the DBO station grid that extends from the northern
221 Bering Sea south of St. Lawrence Island to Barrow Canyon in the northern Chukchi Sea, and,
222 additionally, the Hanna Shoal area in the northeast Chukchi Sea (Fig. 2). Bivalve samples were
223 collected during the cruise of Canadian Coast Guard Ship (CCGS) Sir Wilfrid Laurier in July
224 2015 (SWL2015) at the five DBO sites (Fig. 2, Table 1) that experience different physical forcing
225 and a gradient of seasonal sea-ice cover duration, increasing from south to north. Additional
226 samples were collected in the northeastern Chukchi Sea during a US Coast Guard Cutter
227 (USCGC) Healy (HLY1301) cruise in July/August 2013 as part of the Chukchi Sea Offshore
228 Monitoring in Drilling Area (COMIDA) program, at 14 sampling stations across the Chukchi
229 shelf, extending from the undersea Barrow Canyon feature and including the shallow water area
230 at Hanna Shoal (Fig. 2, Table 1).
231

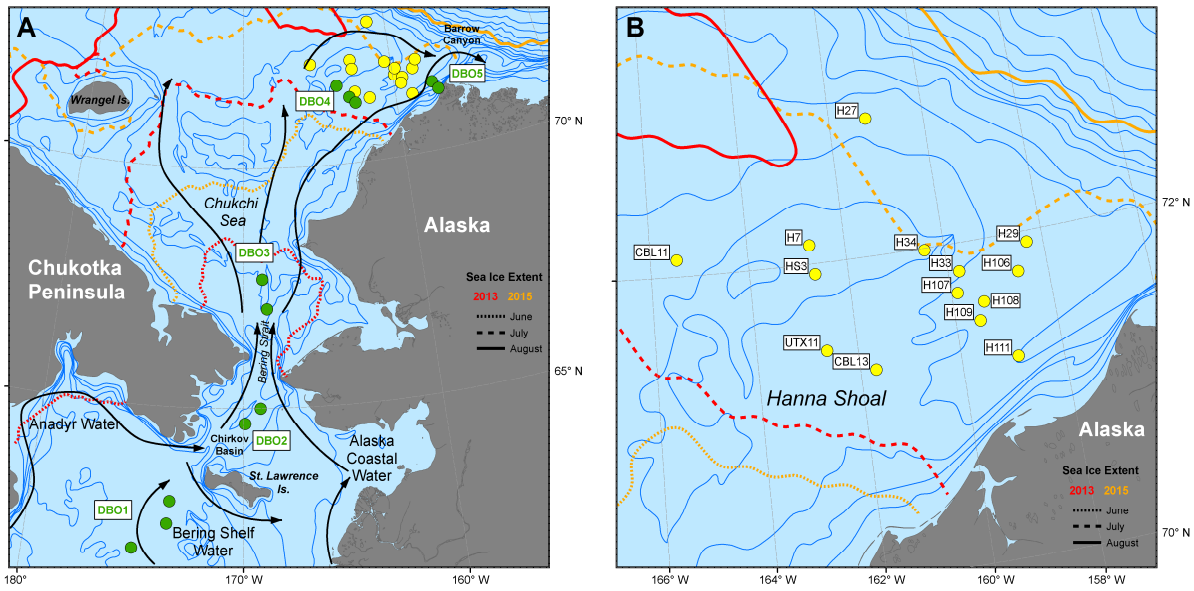

Fig. 2. Location of sampling sites: A - in yellow – stations sampled in 2013 during HLY1301 cruise in the northern Chukchi Sea; in green – stations sampled in 2015 during SWL15 cruise (DBO1 – St. Lawrence Island Polynya, DBO2 – Chirikov Basin, DBO3 - southern Chukchi Sea, DBO4 – northern Chukchi Sea, DBO5 – Barrow Canyon, Hanna Shoal - northeast corner). The black lines and arrows indicate the general flow of the water mass and associated current. B – Larger scale map of station locations sampled in the Hanna Shoal region. The sea-ice extent contour lines for June-July-August in 2013 and 2015 are denoted by red (2013) and orange lines (2015; sea ice extent from Fetterer, et al., 2017).

The bivalve samples were collected using a 0.1 m^2 Van Veen grab from sediments that were washed over a 1 mm sieve. Bivalves were sorted from the sieve, kept cool at ambient temperatures for 24 hours in clean sea water to allow gut clearance, and identified under a stereomicroscope on board. In the case of larger organisms we collected animal's foot while in case of smaller organisms we collected all soft tissue but tried to avoid guts. For Hanna Shoal, in addition to benthic samples, pelagic POM samples, representing a mixture of PP including

248 phytoplankton, detritus, and other particles were collected with a 20 µm mesh and filtered onto
249 25mm Whatman GF/F filters that had been pre-combusted at 450°C for 24 h to remove trace
250 organic material. Similarly, OM recovered from melted sea-ice (IPOM), collected at station H33
251 (71° 41.466 N, 159° 46.329 W) on 10 August 2013, was filtered from the melted sea-ice water
252 (sea-ice cores were thawed in the dark at 4°C). All samples were frozen and shipped to the
253 Chesapeake Biological Laboratory (CBL) in Solomons, Maryland, USA where they were stored
254 in a -20°C freezer prior to processing for compound-specific stable isotope analyses. Bivalves
255 selected for the CSIA-AA included seven dominant bivalve species occurring along the
256 latitudinal gradient in the Bering and Chukchi Seas and two species in the Hanna Shoal (Table 2).
257

258 **Table 1.** Location and basic environmental data for sampling stations.

Cruise	Station group	Latitude [°N]	Longitude [°W]	Depth [m]	Sediment type	T [°C]	S	Sed Chl *a* [mg m^{-2}]	TOC [%]	C/N	Sed $\delta^{13}C$
SWL15	DBO1	62.01–63.03	173.46 – 175.06	66-76	Sandy muds	-1.1 – -0.7	31.7 – 32.2	12.1 - 26.4	1.0 - 1.5	6.1 – 6.5	-21.7 - -21.4
	DBO2	64.7	169.92	48	Sands	3.1	32.7	29.5	0.3	5.8	-20.8
	DBO3	67.05 - 67.67	168.73 - 168.96	46 - 51	Sands, muds	3.4 - 4.7	32.3 - 32.8	17.3 - 20.0	0.6 - 0.9	6.2 - 6.3	-21.5 - -21.2
	DBO4	71.23 - 71.62	162.65 - 163.79	37 - 47	Muds, sandy muds	-1.5 - - 1.3	32.3 - 32.8	7.0 - 18.0	0.01 - 1.0	4.4 - 11.7	-25.4 - -22.4
	DBO5	71.25 71.41	157.49 157.16	47 125	Sands, gravel	-0.5 -1.7	32.4 32.4	24.6 3.9	0.6 1.3	7.1 8.0	-22.6 -23.6
HLY1301	Hanna Shoal	71.2 – 72.8	158.8 – 165.5	38 - 109	Muds, sandy muds, sands and gravel	-1.72 – -1.55	32.6 – 33.2	3.3 – 17.3	0.46 – 1.48	6.28 – 7.59	-24.24 - - 21.9

259

Surface sediments were collected out of a small door at the top of the van Veen grab prior to opening it and subsamples were collected for sediment chlorophyll *a* (chl *a*), total organic carbon, grain size, and the $\delta^{13}C$ values of the bulk organic content of the surface sediments. Sediment chl *a* was measured shipboard using methods described in Cooper, et al. (2002). Other surface sediment subsamples were stored frozen and returned to CBL for analytical processing using standard grain size, total organic carbon and stable carbon isotope methods as described elsewhere (e.g. Grebmeier, et al. 2015b; Cooper and Grebmeier, 2018). Results for these sediment parameters are provided in those publications. Samples were also assayed for bulk carbon isotope composition, as well as TOC and C/N weight/weight ratios, using standard methods that involved organic tissue combustion in an elemental analyzer coupled to stable isotope mass spectrometer.

2.3. Compound-specific stable isotope analysis

Sample preparation generally followed standard methods (Macko and Uhle, 1997; Silfer, et al., 1991). Approximately 5-10 mg animal tissues and up to 20 mg of POM samples were homogenized, weighed (dry weight), and acid hydrolized in 0.5 mL of 6N HCl in vials flushed with nitrogen gas at 110°C for 20 hours to extract AAs from proteinaceous components. The remaining acid was evaporated at 55°C under a N_2 stream and the residue was then re-dissolved by adding 1 mL of 0.01N HCl and purified by cation ion exchange. The dried residue was re-dissolved by adding 0.5 mL of 0.2N HCl to each vial. In an ice bath, 2.5 mL of a chilled 4:1 isopropanol and acetyl chloride mixture was added, the vials were flushed with N_2 and then

283 heated at 110°C for 1 hour. After heating, samples were cooled to room temperature and dried
284 under a stream of N_2 at 60°C. The residue was re-dissolved in 0.6 mL HPLC grade methylene
285 chloride and dried under a stream of N_2 at room temperature. Subsequently, each vial with a
286 sample was filled with an additional 1.5 mL of methylene chloride, followed by the addition of
287 0.5 mL of trifluoroacetic anhydride (TFAA). The vials were flushed with N_2 and heated at 110°C
288 for 15 minutes, and then cooled to room temperature. The derivatized product was dried at room
289 temperature under a stream of N_2. The vials were filled again with 0.6 mL of methylene chloride
290 and dried under a stream of N_2, and this rinse was repeated twice to remove any remaining
291 reactants. The final product was dissolved in 1 mL methylene chloride and stored in the freezer (-
292 20°C).

293 Derivatized AAs standards and samples were analyzed using a Thermo Trace Ultra gas
294 chromatograph interfaced with a Thermo Delta V Plus isotope ratio mass spectrometer (GC-
295 IRMS). For each sample one mL of derivatized product was equally divided into two parts, one
296 for carbon isotope analysis and the other for nitrogen isotope analysis (Kędra, et al., 2019). For
297 carbon isotope analysis, a 0.5 mL aliquot of the product was diluted by adding 1 mL of
298 methylene chloride. A 2 µL AA solution was injected onto a BPX5 capillary column (60m ×
299 0.32mm × 1.0µm film thickness; SGE Analytical Services, Austin, Texas, USA) at an injection
300 temperature of 180°C using a split/splitless injector (in splitless mode) with a constant helium
301 flow rate of 2.0 mL min^{-1}. The column was held at an initial temperature of 75°C for 2 min;
302 ramped up to 90°C at 4°C min^{-1}, held for 4 min; ramped to 185°C at 4°C min^{-1}, held for 5 min;
303 ramped to 250°C at 10°C min^{-1}, held for 2 min; and finally ramped to 300°C at 20°C min^{-1}, and
304 held for 8 min.

305 The separated AAs were combusted in a GC Isolink at 980 ºC, which converts AAs to
306 CO_2 and N_2, and passed through a Thermo Conflo IV continuous flow interface, with the isotope
307 composition of the individual AAs measured on the isotope ratio mass spectrometer. Twelve to
308 thirteen individual AAs identified had sufficient baseline separation to permit identification.
309 CSIA-AA samples were analyzed along with AA standards of known isotopic composition (Gly,
310 Phe and Val; source: Indiana University; http://pages.iu.edu/~aschimme/compounds.html) that
311 were derivatized in batches with the samples. Individual samples were analyzed three times and
312 the mean analytical error for all derivatized amino acids was ±0.5‰.
313
314 *2.4. Standardization and corrections for derivatization*
315
316 A correction is necessary post-analysis to the stable carbon isotope composition of the
317 individual $\delta^{13}C_{AA}$ values because of contributions of carbon in the reagents used during
318 processing and the size of the correction is dependent upon the structure of each AA. The
319 correction that is applied for the carbon atoms added during derivatization and the kinetic
320 fractionations associated with esterification and alkylation (Silfer et al. 1991) uses a linear
321 regression approach (Docherty et al. 2001; Howland et al. 2003), that regresses the known
322 isotopic composition of the AA standards (using the standards from Indiana University) as
323 measured following direct combustion by elemental analyzer and without derivatization to the
324 isotopic composition following derivatization:

325 $$p\delta^{13}C_{der} = m\delta^{13}C_{AA} + n\delta^{13}C_{rea}$$

326 $$p = m + n$$

$$\theta = \frac{m}{p}$$

$$\delta^{13}C_{der} = \theta\delta^{13}C_{AA} + (1-\theta)\delta^{13}C_{rea}$$

$\delta^{13}C_{der}$, $\delta^{13}C_{AA}$, $\delta\ ^{13}C_{rea}$ refer to the carbon isotopic composition of the derivatized product, underivatized AA and derivatizing reagents, respectively. The variables p, m, and n refer to the number of carbon atoms in a molecule of a derivatized product, the number of carbon atoms originating from underivatized AA molecules and that added from derivatizing reagents, respectively. θ refers to the ratio of the number of carbon atoms in each molecule originating from underivatized AA to the total number of carbon atoms in each molecule of the derivatized product, which vary in different AAs. For all AAs, the relationship between the carbon isotope compositions of original AAs and their derivative product is:

$$\delta^{13}C_{der} = \theta\delta^{13}C_{AA} + (1-\theta)\delta^{13}C_{rea}$$

which can be rewritten as:

$$\frac{1}{1-\theta}\delta^{13}C_{der} = \frac{\theta}{1-\theta}\delta^{13}C_{AA} + \delta^{13}C_{rea}$$

meaning that the measured carbon isotopic values of derivatized product and the known isotopic values of standards obtained from Indiana University are fitted to a linear regression model of the form:

$$\boldsymbol{Y} = a\boldsymbol{X} + b, \text{where}$$

$$\boldsymbol{Y} = \frac{1}{1-\theta}\delta^{13}C_{der};\ \boldsymbol{X} = \frac{\theta}{1-\theta}\delta^{13}C_{AA};\ a \approx 1;\ b = \delta^{13}C_{rea} + b_0$$ (b_0 is the term of error)

346 $$Y = 0.9951X - 27.388$$

347 Based upon the linear regression model obtained, Y = 0.9951X - 27.388 (r^2 = 0.99), as
348 well as θ calculated for each AA (θ = m/p), we then calculated the carbon isotopic values of the
349 original AAs ($\delta^{13}C_{AA}$) based on the measured carbon isotopic values of the derivatized AAs
350 ($\delta^{13}C_{der}$):

351 $$\frac{1}{1-\theta}\delta^{13}C_{der} = a\frac{\theta}{1-\theta}\delta^{13}C_{AA} + b$$

352 $$\delta^{13}C_{AA} = \frac{1-\theta}{a\theta}(\frac{1}{1-\theta}\delta^{13}C_{der} - b)$$

353 $$a = 0.9951; b = -27.388$$

354

355 *2.5. Data analysis*

356

357 Carbon isotopic composition of individual AAs ($\delta^{13}C_{AA}$) are given as means with
358 standard deviations where replicates were available. We compared CSIA-AA patterns in different
359 samples by normalizing the data to the average of essential AAs $\delta^{13}C$ (normalized $\delta^{13}C_{AA}$ =
360 measured $\delta^{13}C_{AA}$-essential AAs $\delta^{13}C_{Avg}$). This normalization approach allows direct assessment
361 of biosynthetic signatures by removing any variability associated with changes in baseline $\delta^{13}C$
362 between samples (Vokhshoori, et al., 2014). We used an AA isotope fingerprinting approach
363 (Larsen, et al., 2009, 2013) to identify the probable composition of carbon sources fueling
364 benthic bivalve production in Hanna Shoal and the DBO sites. We performed linear discriminant
365 function analysis (LDA) to identify patterns of essential AAs that are best suited to separate
366 bacteria, microalgae, and terrestrial plants using literature data from Larsen, et al. (2013) as a

training set. We selected bacteria, microalgae, and terrestrial plants as potential carbon sources, as they have been identified as carbon sources contributing significantly to *Macoma* spp . and *Astarte* spp. in Hanna Shoal (Rowe, et al., 2019). The choice of these three potential sources is also supported by knowledge of the marine ecosystems and benthic feeding behavior: microalgae (phytoplankton, sea-ice algae) and bacteria (bacterially reworked OM, detritus) are commonly used by benthic species (e.g. Lovvorn et al., 2005, North et al., 2014). Since the location of sampling sites is not far from land we also decided to take into account terrestrial OM as potential food source (as also accounted for by Iken et al., 2010, McTigue et al., 2015). We used a predictive function to assign all IPOM, POM, and bivalve samples to one of the three carbon sources. The function assigns each sample to the nearest carbon source centroid weighted by the proportion of variance explained by each axis (Tabachnick and Fidell, 2013). To quantify the relative contribution of the different carbon sources to IPOM, POM, and bivalves, we analyzed normalized essential AA data using the MixSIAR framework (Stock and Semmens, 2016) with Sampling location and Species identity as fixed effects. In recent years, MixSIAR has become one of the major tools to analyze biotracer (i.e. stable isotopes, fatty acids) data, as it allows for the use of any number of biotracers. Furthermore, it uses a Bayesian Mixing model to analyze the biotracer data, which is particularly beneficial in ecology as it incorporates parameter (source and consumer) variability in the estimated source proportions (Parnell et al. 2010). We followed the approach of Larsen, et al. (2013), Elliott Smith, et al. (2018), and Rowe, et al. (2019) and assumed no fractionation of $\delta^{13}C$ in essential AA and accordingly all discrimination factors in the mixing model were set to 0. The same literature data as in the LDA were used as sources in the mixing model (expressed as mean and sd), which was run on the "very long" setting (i.e., chain length = 1,000,000; burn = 500,000; thin = 500; chains = 3) with an uninformative prior. Gelman-Rubin diagnostics and Geweke diagnostics were used to verify that the model had

converged. Furthermore, posterior distributions of the three chains were visually compared with each other to ensure that all chains produced almost identical results (Silberberger, et al., 2021). Since normalized Phe values of our samples behaved differently in relation to carbon sources compared to all other essential AAs, LDA and MixSIAR analysis were performed twice: (i) on the full normalized EAA data and (ii) with Phe excluded. LDA and Bayesian mixing model were performed in R, version 3.5.1 (R Development Core Team, 2018). No test to identify significant differences between sampling locations and species was conducted due to insufficient number of replicates.

3. Results

We quantified $\delta^{13}C$ values of 7 non-essential AAs (Ala, Gly, Ser, Pro, Asp, Glu, Tyr) and 6 essential AAs (Thr, Val, Leu, Iso, Phe, Lys) for 8 samples of POM, 3 samples of IPOM, and 21 samples of two bivalve species: *Macoma calcarea* (Gmelin, 1791) and *Ennucula tenuis* (Montagu, 1808) collected over the Hanna Shoal area. One additional essential AA (Met) was measured for 25 samples of 7 bivalve species collected along the DBO hot spot sites in the northern Bering and Chukchi Seas (Table 2, Fig. 3). We excluded Tyr and Met from the statistical analysis due to limited and missing measurements.

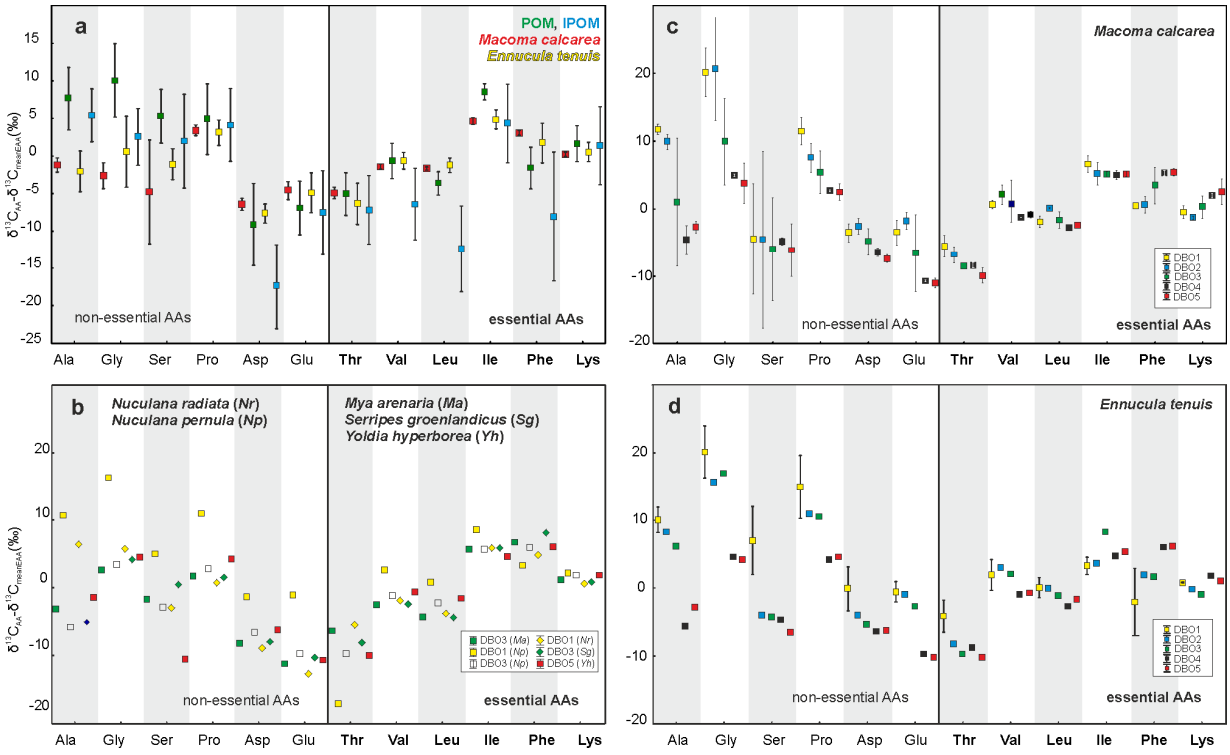

Fig. 3. Normalized $\delta^{13}C$ values ($\delta^{13}C_{AA}$-$\delta^{13}C_{meanEAA}$) of individual AAs of: a - pelagic particulate organic matter (POM) and melted sea-ice OM (IPOM), and bivalve species: *Macoma calcarea* and *Ennucula tenuis* collected around Hanna Shoal in the northern Chukchi Sea, and select bivalve species: b - *Nuculana radiata (Nr)*, *N. pernula (Np)*, *Mya arenaria (Ma)*, *Serripes groenlandicus (Sg)*, *Yoldia hyperborea (Yh)*, c - *Macoma calcarea*, d - *Ennucula tenuis*, collected in the northern Bering and Chukchi Seas along DBO sites. Individual values in case of single measurements or means are presented with standard errors. Ala – alanine, Gly – glycine, Ser – serine, Pro – proline, Asp – aspartic acid, Glu – glutamic acid, **Thr** – threonine, **Val** – valine, **Leu** – leucine, **Ile** – isoleucine, **Phe** – phenylalanine, **Lys** – lysine. **Essential AAs** are indicated by **bold** print.

Table 2. $\delta^{13}C_{Bulk}$ and $\delta^{13}C_{AA}$ values of selected food sources and selected bivalve species collected the northern Bering and Chukchi Seas (DBO – SWL15 cruise, and Hanna Shoal (HS) – HLY1301 cruise). POM – Particulate Organic Matter collected from the water column (phytoplankton), IPOM – and melted sea-ice Organic Matter. **Phe** – phenylalanine, **Thr** – threonine, **Ile** – isoleucine, **Leu** – leucine, **Val** – valine, **Lys** – lysine, Asp – aspartic acid, Glu – glutamic acid, Pro – proline, Ala – alanine, Ser – serine, Gly – glycine, Tyr – tyrosine. **Essential AAs** are indicated by **bold** print.

Taxon/ Station	No of samples	$\delta^{13}C_{Bulk}$	**Essential $\delta^{13}C_{AA}$**							Non-essential $\delta^{13}C_{AA}$						
			Phe	**Thr**	**Ile**	**Leu**	**Val**	**Lys**	**Met**	Asp	Glu	Pro	Ala	Ser	Gly	Tyr
POM																
HS	8		**-31.1 ± 4.1**	**-34.6 ± 2.8**	**-21.0 ± 2.2**	**-33.1 ± 2.6**	**-30.2 ± 2.8**	**-27.8 ± 2.5**		-38.6 ± 5.9	-36.4 ± 3.7	-24.6 ± 4.1	-21.9 ± 3.6	-24.2 ± 3.7	-19.5 ± 5.1	-19.2 ± 2.0
IPOM																
HS	3		**-35.1 ± 5.5**	**-34.2 ± 1.7**	**-22.7 ± 2.0**	**-39.4 ± 2.6**	**-33.5 ± 1.6**	**-25.6 ± 2.1**		-44.5 ± 2.4	-34.6 ± 2.6	-22.9 ± 2.1	-19.6 ± 1.1	-25.1 ± 3.8	-24.5 ± 0.7	-17.0 ± 3.7
Suspension feeders																
Mya areanaria																
DBO3	1	-17.8	**-12.6**	**-25.7**	**-13.6**	**-23.7**	**-21.9**	**-18.2**	**-14.9**	-27.5	-30.5	-17.6	-22.6	-21.1	-16.8	-28.7
Serripes groenlandicus																
DBO3	1	-17.3	**-10.1**	**-27.1**	**-13.2**	**-23.5**	**-21.5**	**-18.2**	**-14.7**	-27.1	-29.4	-17.5	-24.1	-18.6	-14.9	-29.8
Surface deposit feeders																
Macoma calcarea																
DBO1	4	-20.3 ± 1.9	**-28.0 ± 0.2**	**-34.1 ± 1.5**	**-21.9 ± 1.4**	**-30.4 ± 0.9**	**-27.9 ± 0.8**	**-29.0 ± 0.9**	**-16.5 ± 1.6**	-32.1 ± 1.5	-32.1 ± 1.8	-17.1 ± 1.8	-16.8 ± 1.0	-33.0 ± 7.6	-8.4 ± 3.5	
DBO2	2	-17.0 ± 0.3	**-23.4 ± 2.1**	**-30.8 ± 0.4**	**-18.8 ± 0.1**	**-23.9 ± 1.1**	**-21.9 ± 2.2**	**-25.3 ± 1.4**	**-11.4 ± 0.9**	-26.6 ± 2.0	-25.7 ± 2.1	-16.5 ± 0.3	-14.1 ± 0.4	-28.6 ±8.0	-3.4 ± 4.2	
DBO3	2	-17.2 ± 0.5	**-17.7 ± 4.7**	**-29.6 ± 2.5**	**-16.0 ± 3.1**	**-22.7 ± 1.9**	**-19.9 ± 0.6**	**-20.8 ± 4.0**	**-11.7 ± 1.1**	-26.0 ± 1.4	-27.7 ± 1.3	-15.7 ± 0.6	-20.2 ± 3.9	-27.1 ±8.2	-11.2 ± 1.7	
DBO4	2	-20.6 ± 2.1	**-13.9 ± 0.1**	**-27.5 ± 0.7**	**-14.1 ± 0.1**	**-21.9 ± 0.6**	**-20.4 ± 0.4**	**-17.2 ± 0.6**	**-14.0 ± 0.3**	-25.6 ± 0.0	-29.9 ± 0.5	-16.5 ± 0.5	-23.8 ± 1.9	-24.0 ± 0.0	-14.2 ± 0.5	-27.3 ± 1.8

DBO5	2	-21.1 ± 1.3	**-14.3 ± 0.1**	**-29.6 ± 0.5**	**-14.6 ± 0.0**	**-22.2 ± 0.1**	**-20.6 ± 0.7**	**-17.2 ± 1.6**	**-14.4 ± 1.0**	-27.1 ± 0.1	-30.7 ± 0.2	-17.2 ± 0.6	-22.4 ± 0.9	-25.8 ± 3.1	-15.9 ± 2.4	-27.3 ± 1.2
Hanna Shoal	11		**-18.4 ± 0.6**	**-26.4 ± 1.5**	**-16.9 ± 0.7**	**-23.2 ± 0.7**	**-22.9 ± 0.8**	**-21.3 ± 0.8**		-28.0 ± 1.5	-26.1 ± 1.7	-18.1 ± 1.0	-22.7 ± 1.5	-26.3 ± 7.2	-24.1 ± 2.4	-15.3 ± 0.9
Yoldia hyperborea																
DBO1	1	-18.6	**-14.2**	**-30.3**	**-15.6**	**-21.9**	**-20.9**	**-18.4**	**-14.0**	-26.4	-30.9	-16.0	-21.8	-30.8	-15.8	-26.3
Subsurface deposit feeders																
Ennucula tenuis																
DBO1	3	-18.8 ± 0.5	**-28.5 ± 4.5**	**-30.6 ± 2.0**	**-23.1 ± 2.1**	**-26.3 ± 1.3**	**-24.5 ± 2.0**	**-25.6 ± 1.3**	**-12.2 ± 1.2**	-26.5 ± 2.9	-27.0 ± 1.0	-11.5 ± 2.8	-16.4 ± 0.5	-19.4 ± 3.5	-6.3 ± 1.8	
DBO2	1	-18.4	**-22.6**	**-32.8**	**-20.9**	**-24.6**	**-21.6**	**-24.8**	**-10.8**	-28.5	-25.5	-13.6	-16.3	-28.6	-8.9	
DBO3	1	-17.8	**-21.2**	**-32.6**	**-14.7**	**-24.0**	**-20.8**	**-23.9**	**-10.0**	-28.2	-25.6	-12.4	-16.7	-27.2	-6.0	
DBO4	1	-21.0	**-12.7**	**-27.4**	**-14.0**	**-21.5**	**-19.6**	**-16.9**	**-12.7**	-25.1	-28.3	-14.5	-24.2	-23.4	-14.1	-28.0
DBO5	1		**-14.3**	**-30.7**	**-15.1**	**-22.1**	**-21.1**	**-19.4**	**-13.9**	-26.7	-30.6	-15.9	-23.3	-27.0	-16.3	-27.6
HS	10		**-20.9 ± 3.2**	**-29.0 ± 2.8**	**-17.8 ± 0.9**	**-23.9 ± 1.0**	**-23.3 ± 0.8**	**-22.1 ± 1.1**		-30.3 ± 1.3	-27.5 ± 3.2	-19.5 ± 1.8	-24.7 ± 2.5	-23.7 ± 2.3	-22.1 ± 4.2	-16.0 ± 0.5
Nuculana pernula																
DBO1	1	-21.4	**-24.2**	**-44.6**	**-18.9**	**-26.7**	**-24.8**	**-25.2**	**-14.1**	-28.8	-28.5	-16.5	-16.7	-22.5	-11.1	
DBO3	1	-17.9	**-13.3**	**-29.1**	**-13.6**	**-21.5**	**-20.4**	**-17.5**	**-12.9**	-25.8	-29.0	-16.5	-25.2	-22.2	-15.9	-28.1
Nuculana radiata																
DBO1	1	-18.5	**-14.3**	**-24.5**	**-13.2**	**-23.0**	**-21.0**	**-18.4**	**-14.5**	-28.0	-31.8	-18.4	-12.6	-22.1	-13.3	-30.7

430 The $\delta^{13}C_{AA}$ values from POM samples and samples derived from organic materials in
431 melted sea-ice (IPOM) displayed consistent patterns over the Hanna Shoal area: the non-essential
432 AAs - Glu and Asp, as well as the essential AAs – Val, Leu, Thr, Phe, were typically more
433 depleted in ^{13}C than the other AAs (Fig. 3, Table 2). The essential $\delta^{13}C_{AA}$ values derived from
434 IPOM were similar to POM, except for Leu, which was more depleted in ^{13}C than the values
435 observed in POM. The $\delta^{13}C_{AA}$ values in *M. calcarea* tissue were more depleted in ^{13}C at four
436 locations near 71°N 161°W (Hanna Shoal stations H34, H33, H106 and H107) and one other
437 location to the north (H27). Bivalves collected at other nearby stations gradually became
438 relatively enriched in ^{13}C to the west and east. Bivalves collected at the DBO sites had generally
439 lower non-essential $\delta^{13}C_{AA}$ values to the south (Fig. 3, Table 2).
440

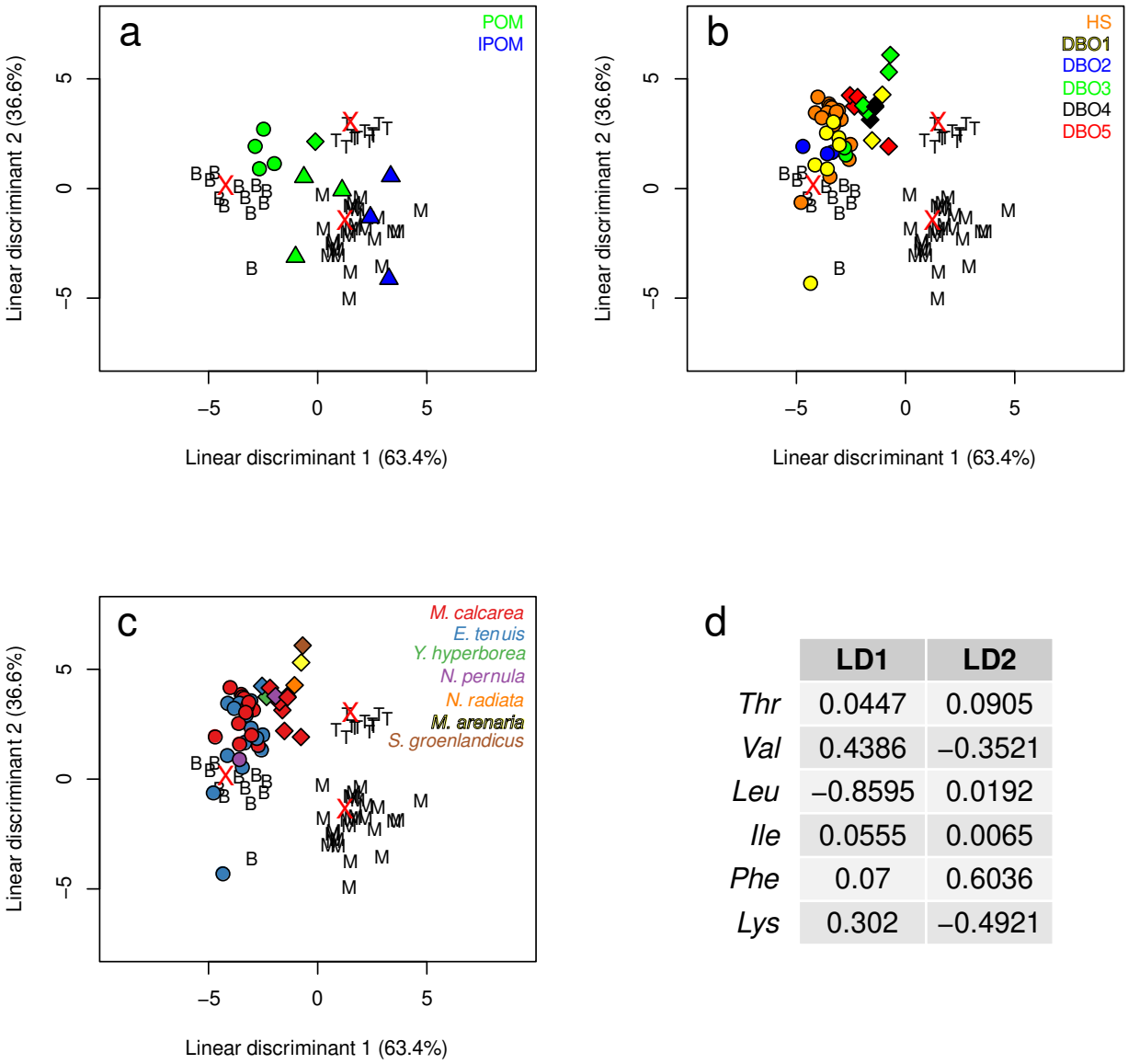

d

	LD1	LD2
Thr	0.0447	0.0905
Val	0.4386	−0.3521
Leu	−0.8595	0.0192
Ile	0.0555	0.0065
Phe	0.07	0.6036
Lys	0.302	−0.4921

Fig. 4. Results of the Linear Discriminant Analysis (LDA) based on relationships among $\delta^{13}C_{AA}$ values of all essential AAs. The LDA plot with bacterial (B), microalgal (M), and terrestrial plant (T) training data using Larsen, et al. (2013) are shown together with a) IPOM and POM samples, b) bivalve samples according to sampling location, and c) bivalve species identity. The red X indicate group centroids. IPOM, POM, and bivalve samples that were classified as having bacteria, microalgae, or terrestrial organic carbon origin are depicted as circle, triangle, or diamond, respectively. d) LDA coefficients of all included essential AAs are given in the table.

449

450 The LDA classified all IPOM samples as microalgae, while most POM samples clustered
451 between the three carbon sources (Fig. 4). All bivalve samples from DBO4 and DBO5 together
452 with 4 samples from DBO3 and 2 samples from DBO1 were assigned to terrestrial OM as carbon
453 source, while the remaining bivalves were assigned to bacteria. The MixSIAR mixing model
454 supported the LDA result of IPOM samples being composed mainly of microalgae (85.6%, Fig.
455 5). Furthermore, it supported a strong reworking of POM samples that contained only 34.1%
456 microalgae. In contrast to the LDA results, the MixSIAR model did not identify any importance
457 for terrestrial plants as a source for POM or ultimately bivalves (Fig. 5). According to the model,
458 most bivalves relied almost exclusively on bacteria-mediated OM. However, *Nuculana radiata*
459 from DBO1 as well as *Mya arenaria* and *Serripes groenlandicus* from DBO3 were identified as
460 having a higher reliance on microalgae than other samples from these stations. Furthermore, the
461 contribution of microalgae to bivalve diet was slightly higher at the northern sampling stations:
462 DBO4, DBO5, and Hanna Shoal. Overall, MixSIAR results differed strongly from the LDA
463 results, especially for samples with a low contribution of microalgae (Fig. 4, 5).

464 We identified this discrepancy between LDA and MixSIAR results as being related to the
465 use of Phe in the analysis. While all other AAs followed a gradient from IPOM to POM to
466 bivalves that was aligned with the gradient from microalgae to bacteria, the same gradient for Phe
467 was aligned with a gradient from microalgae to terrestrial plants. Since Phe had a strong
468 influence on LD2 (Fig. 4), this resulted in the classification of samples as using terrestrial plant
469 organic carbon. When Phe was excluded from the LDA and mixing model (Fig. 6, 7), the
470 observed patterns in both analyses resembled the patterns described for the MixSIAR results of
471 the full essential AA data set (Fig. 5). However, the removal of Phe from the mixing model

increased the overall importance of microalgae for all samples (Fig. 7). With Phe removed from the analysis, LDA and MixSIAR results agreed well (Fig. 6, 7), identifying the northern stations (DBO4 and DBO5), *N. radiata* (DBO1), *M. arenaria* (DBO3), and *S. groenlandicus* (DBO3) as most reliant on microalgae. Bacterially reworked material remains the most important OM source for all studied bivalves.

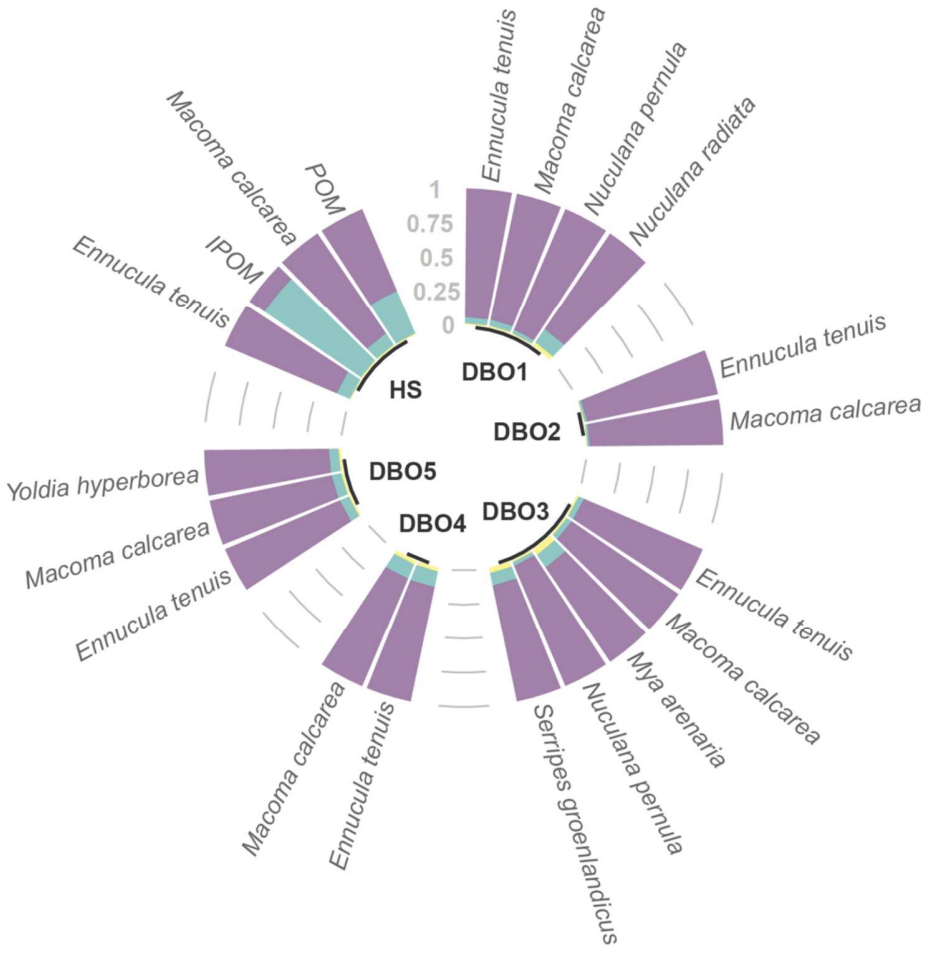

Fig. 5. Results of the Bayesian mixing model (MixSIAR). The relative reliance on terrestrial plants (yellow), microalgae (green), and bacteria (purple) are indicated for each sample type per sampling region. Note: Bars for terrestrial plants are only marginally visible due to their low contribution

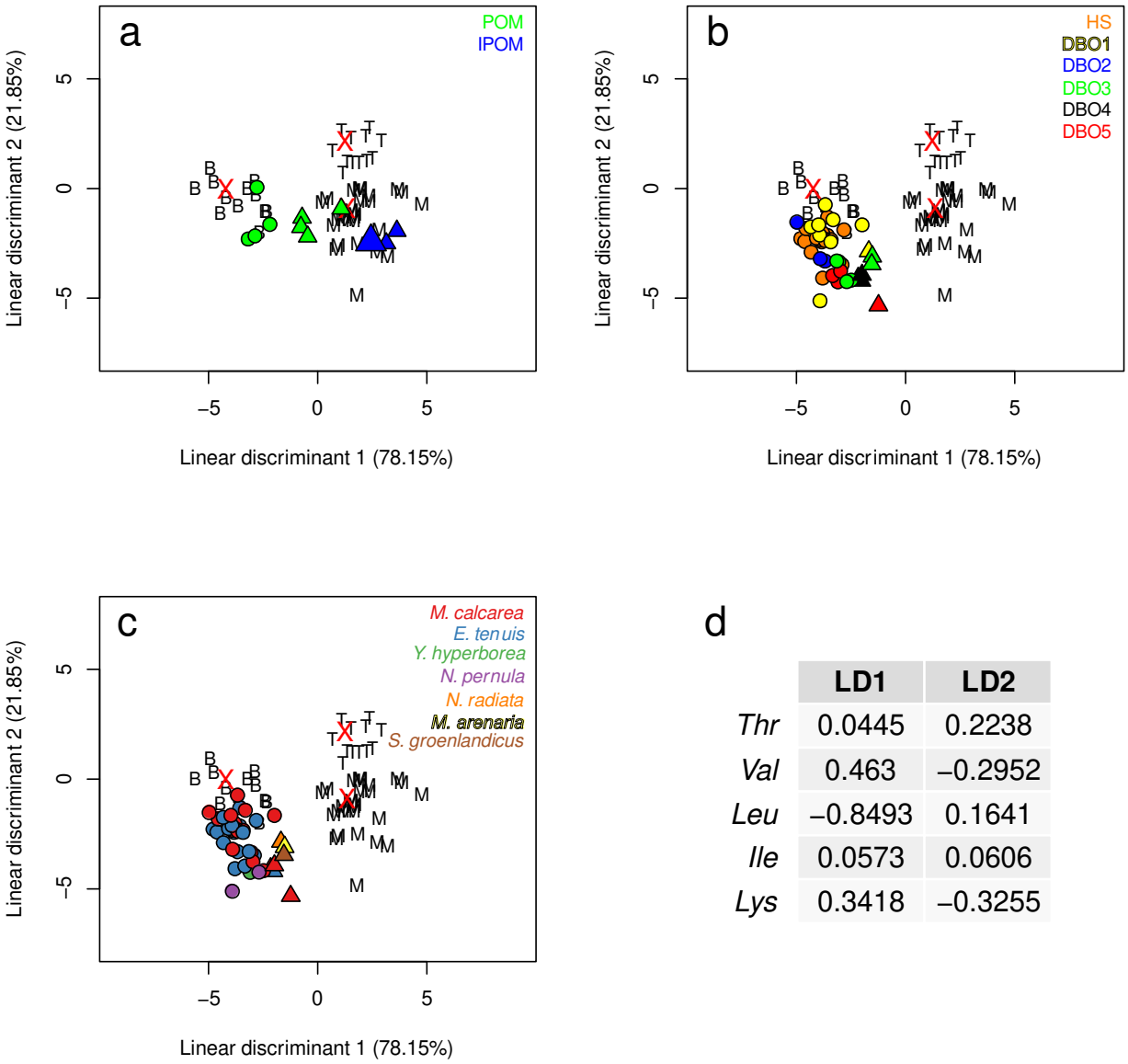

d

	LD1	LD2
Thr	0.0445	0.2238
Val	0.463	−0.2952
Leu	−0.8493	0.1641
Ile	0.0573	0.0606
Lys	0.3418	−0.3255

Fig. 6. Results of the Linear discriminant analysis (LDA) based on $\delta^{13}C_{AA}$ values of essential AAs with Phe excluded. The LDA plot with bacterial (B), microalgal (M), and terrestrial plant (T) training data according to Larsen, et al. (2013) are shown together with a) IPOM and POM samples, b) bivalve samples according to sampling location, and c) bivalve species identity. Red X's indicate group centroids. IPOM, POM, and bivalve samples that were classified as having bacteria, microalgae, or terrestrial organic carbon origins are depicted as circle, triangle, or diamond, respectively. d) LDA coefficients of all included essential AAs are given in the table.

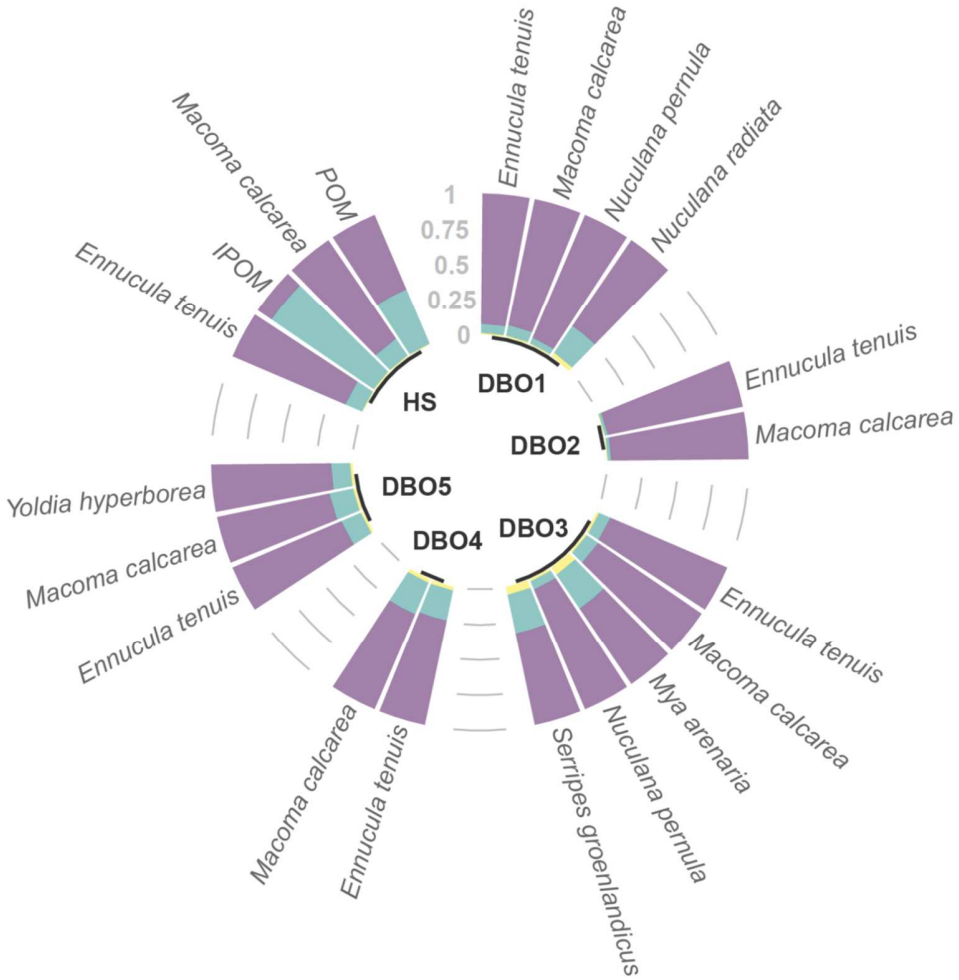

Fig. 7. Results of the Bayesian mixing model (MixSIAR) with Phe excluded from the normalized essential AAs. The relative reliance on terrestrial plants (yellow), microalgae (green), and bacteria (purple) are indicated for each sample type per sampling region. Note: Bars for terrestrial plants are hardly visible due to their low contribution.

4. Discussion

We showed, through the use of CSIA-AA and $\delta^{13}C_{AA}$ patterns, that the relative importance of fresh PP (microalgae) increased with the increasing latitude and sea-ice persistence for two

501 common Pacific shelf bivalve species, *M. calcarea* and *E. tenuis.* This pattern is likely a
502 consequence of higher input of fresh PP (from sea-ice) to the bottom communities in the most
503 northern locations, where sea-ice breaks up later during the year. Specimens collected in the more
504 southern areas, where sea-ice retreats earlier in the year, mainly relied on bacterially reworked
505 OM. This largely confirmed our initial hypothesis (Fig. 1) that the water column production and
506 water column processing, as well as sediment processing of OM, increase in prominence where
507 sea-ice persistence declines. This pattern, with some exceptions, was largely followed by other
508 bivalves collected during this study, particularly by deposit feeders.
509
510 *4.1. Food sources and their spatial variability*
511
512 The two main potential food sources were sampled over Hanna Shoal: pelagic POM and
513 material derived from the sea-ice (IPOM). Although there was a large spatial variability in $\delta^{13}C_{AA}$
514 values for pelagic POM over Hanna Shoal the majority of these samples seem to be mixtures of
515 phytoplankton, bacteria, and bacterially reworked microalgal organic carbon. The LDA and
516 mixing model results (Phe excluded) pointed to marine and bacterial sources as the main
517 composition of both POM and IPOM, while terrestrial plants did not contribute significantly
518 (<1%). Furthermore, the mixing model showed that IPOM mainly consisted of microalgae while
519 POM consisted of mixture of microalgae (42%) and bacteria (57%). It is likely that, due to the
520 timing of the sampling (late summer) the POM collected represented to large extent degraded
521 OM including also zooplankton fecal pellets and bacteria. The material collected from the sea-ice
522 seems to be less degraded with a much smaller fraction (12%) of bacteria and the dominance of
523 microalgae (87%), presumably sympagic taxa. Since we do not have essential $\delta^{13}C_{AA}$ values for

524 sea-ice specific microalgae to incorporate into the model, nor did we collect *in situ* pelagic
525 phytoplankton species, we cannot determine the exact composition of those two food sources.
526 The particulate organic carbon export fluxes in the northern Bering and Chukchi Seas are
527 mostly composed of freshly produced labile material (Lalande, et al., 2007; 2020), including
528 phytoplankton and sea-ice algae in the spring, which rapidly arrives to the sea floor and later
529 becomes available to the benthic communities in the form of phytodetritus (Fig. 1; Cooper, et al.,
530 2005; Roca-Martí et al., 2016). Phytoplankton and bacteria are among the primary carbon sources
531 for benthic fauna in the Chukchi Sea (McTigue and Dunton, 2014) although sea-ice algae – when
532 available - are also commonly used by benthic fauna (Koch, et al., 2020). Detritus represents an
533 important carbon pool in marine sediments, but during decomposition, microbial processing of
534 OM causes carbon isotope variation that remains challenging to characterize (Larsen, et al., 2015;
535 McCarthy, et al., 2004). Microbial reworking of fresh OM, sinking particles and microbial
536 processes in the sediments provide for the contribution of new AAs via microbial *de novo*
537 synthesis (including substantial changes in the isotopic composition of AAs). This is an important
538 and seasonally variable process affecting OM composition in aquatic ecosystems (Larsen, et al.,
539 2013, 2015; Ziegler and Fogel, 2003). The $\delta^{13}C$ values of essential AAs in different marine
540 source end members vary significantly (Larsen, et al., 2013; McMahon, et al., 2016) and are
541 reflected in the essential $\delta^{13}C_{AA}$ values of consumers. Since plants, algae and bacteria are able to
542 synthesize essential AAs *de novo*, the $\delta^{13}C$ values of consumers' essential AAs must represent
543 the isotopic fingerprint of primary producers at the base of the food web (Larsen, et al., 2013;
544 McMahon, et al., 2010). Thus, essential $\delta^{13}C_{AA}$ values of detritivores would differ from the
545 patterns of organisms feeding directly on fresh phytoplankton or ice algae. In this study we
546 sampled suspension and deposit feeders and we expected that their essential $\delta^{13}C_{AA}$ patterns
547 should follow a mixed food source pattern, including microalgae (phytoplankton and/or ice

548 algae), or bacteria via detrital processes, or mixtures (POM, IPOM). Our observations of the
549 essential $\delta^{13}C_{AA}$ patterns are consistent with these mixed food sources, with most of the sampled
550 bivalves showing significant reliance on bacterially modified detritus with a general decreasing
551 trend northwards, and secondary use of microalgae that was the highest in suspension feeding *M.*
552 *arenaria* and *S. groenlandicus*.

553 The carbon fingerprinting results are also consistent with the patterns observed in the
554 values of essential $\delta^{13}C_{AA}$, particularly for Ile, Val and Leu, which are specifically associated
555 with bacterial resynthesis of AAs in OM (Keil and Fogel, 2001, McCarthy, et al., 2007). Both Ile
556 and Val synthesized by bacteria are more depleted in ^{13}C than when synthesized by plants
557 (McCarthy, et al., 2007) and conversely Leu becomes relatively more enriched in ^{13}C (Larsen, et
558 al. 2009). In our study, more negative $\delta^{13}C_{AA}$ values for Ile and Val, and less negative $\delta^{13}C_{AA}$
559 values for Leu occurred in all sampled bivalves – both of these trends are consistent with
560 bacterial reworking of utilized OM. High reliance on reworked OM was also shown by Kędra et
561 al. (2019) with use of $\delta^{15}N_{AA}$ values and the degradation ΣV parameter (McCarthy et al., 2007)
562 which had higher values in the deposition areas (DBO1, 3 and 4) in comparison to areas with
563 high currents and potentially higher abundance of fresh OM (DBO2, 5). High contributions of
564 phytoplankton and bacteria were also found with the fingerprinting method for two bivalve taxa:
565 *Astarte* spp. and *Macoma* spp. in Hanna Shoal (Rowe et al., 2019).

566 In addition to the two main OM sources, terrestrial OM was identified as a small and in
567 most respects a negligible source for the bivalve species found in all sampling sites. The highest,
568 but still very small contribution, was found for suspension feeders in DBO3 area, which is a
569 deposition zone with muddy sediments and a high level of OM deposition (Grebmeier and
570 Cooper, 2014). As the suspension feeding mechanism of *Serripes* spp.and *Mya* spp. is not highly

571 selective it is possible that some terrestrial OM can be ingested on regular basis but does not
572 become a dominant source.
573
574 *4.2. Species-specific and latitudinal* $\delta^{13}C_{AA}$ *patterns*
575
576 In addition to our results that suggest that the sampled bivalve species in the Pacific Arctic
577 primarily utilize a mixture of microalgae (phytoplankton, sea-ice algae) and bacteria, largely in
578 the form of detritus and reworked phytoplankton material, additional analysis can be directed
579 towards sampling locations, and to less extent, among species. The LDA and mixing model
580 results showed that essential $\delta^{13}C_{AA}$ patterns in organisms were in part differentiated by feeding
581 behavior, and utilization of various sources of OM that depended on the location. Therefore,
582 location, and thus the environmental conditions influencing local production and decomposition
583 processes, also seem to be important factors shaping the utilization of food resources.
584 Different use of resources in the St. Lawrence Island Polynya (DBO1) and southern Chukchi
585 Sea (DBO3) may have consequences for ecosystem functioning. *Nuculana radiata*, a subsurface
586 deposit feeder, is the main food item for the spectacled eiders in the DBO1 northern Bering Sea
587 area (Lovvorn, et al., 2003; Richman and Lovvorn, 2003; Cooper, et al., 2013). It has been slowly
588 replaced by other clams recently, especially by another subsurface deposit feeding clam, *E.*
589 *tenuis,* that is not normally consumed by diving seaducks (Lovvorn, et al. 2005; Goethel, et al.,
590 2019; Grebmeier, et al., 2015a, b; 2018). Large sized *S. groenlandicus* becomes an important
591 food item for walruses in the Chukchi Sea (Sheffield and Grebmeier, 2009). The population of
592 this high respiration rate species has been increasing over the last decade in the southern Chukchi
593 Sea, up until 2018, when the population crashed due to anoxia, presumably a result of high
594 organic matter export (J. Grebmeier, unpublished data). A recent study by Koch et al. (2020)

595 conducted in the same area with use of highly branched isoprenoid biomarkers also showed that
596 deposit feeding *Macoma* and *Ennucula* spp. incorporated higher levels of sea-ice algae in their
597 diet while the diet of suspension feeders like *Mya* and *Serripes* spp. depended only upon small
598 proportions of sea-ice algae. Although this remains speculative at this point due to sampling in
599 only one season, our results (e.g. DBO1, 3 in Fig. 6) suggest that increased availability of fresh
600 microalgal food to the benthos over the year could be responsible for the recently observed
601 changes in benthic community patterns. *S. groenlandicus* as a suspension feeder and species
602 relying on microalgae for more than 25% of its diet (as does *M. arenaria*) can directly benefit
603 from these changes. *N. radiata*, on the other hand, appears to be the only one of the sampled
604 deposit feeders in the northern Bering Sea (DBO1) that utilizes both microalgae and bacteria
605 (microbially degraded OM), which may be related to its dependence on early season PP and
606 export to the benthos that is subsequently limited in summer due to strong stratification. This
607 results in the species using more microbially degraded OM as the season progresses. Along with
608 increasing sea-water temperatures and decreasing sea-ice cover (Frey, et al., 2018; Grebmeier, et
609 al., 2018), an earlier onset of PP (Hill, et al., 2018) and increased phytoplankton PP is observed in
610 the northern portion of DBO1 and DBO3 (Goethel, et al., 2019; Grebmeier, et al., 2018).
611 Suspension feeders may directly benefit from the new conditions, although with variable impacts
612 over the season. *N. radiata*, on the other hand, may not benefit as it seems to rely on recycled OM
613 with bacterial components (compared to *Serripes*) and despite increased PP in the area, the
614 availability of fresh microalgae may not increase over the long term. The reason is that microbial
615 reworking is expected to increase along with the temperature increase and shifts in the food webs
616 (e.g. Kędra, et al., 2015), and have direct impacts on the different bivalve species populations in
617 the area.

618 We expected that the fresher and less altered organic carbon would be utilized in the northerly
619 sites, where, due to the bloom timing, fresher OM with possible input of ice algae should be
620 available, while in the southern locations (DBO1-2) we expected utilization of more reworked
621 OM with a larger input of bacterial production (Fig. 1). Our results for *M. calcarea* and *E. tenuis,*
622 the two species collected over the whole study area, showed that this latitudinal pattern was
623 confirmed, with some exceptions and was largely followed by other species sampled in the study.
624 This may indicate that the food (carbon) source utilized changes depending on what is available
625 in the ecosystem. The results of the LDA and Bayesian isotopic mixing approach strongly
626 indicate that the importance of detritus (bacteria) decreased in the diet of *M. calcarea* and *E.*
627 *tenuis* at more northerly latitudes, with the exception of Hanna Shoal, where there were local
628 variations, and DBO2, where almost no microalgae were utilized. This pattern was followed by
629 other sampled species with the exception of *N. radiata* at DBO1 and suspension feeders at
630 DBO3, which all had higher contributions of microalgae than other species.
631 This location separation between southern (DBO 1 and 2, with small microalgae contribution)
632 and northern locations (DBO4 and 5, with higher microalgae contribution) for *M. calcarea* and *E.*
633 *tenuis*, suggests that different environmental conditions influence utilization of food sources in
634 DBO1-2 and DBO4-5. The DBO1 area is the most southern location in our study, meaning that
635 the spring bloom occurred here the earliest and more time has passed by the time of sampling
636 since the fresh OM input reached the sea floor. This could lead to a greater degree of microbial
637 degradation, at least relative to other DBO sites. North, et al. (2014) concluded that fresh
638 microalgae contribution to the diet of deposit feeders in the St. Lawrence Island Polynya (DBO1)
639 is small. They suggested that benthic species in DBO1 primarily depend upon heterotrophic
640 microbes, microbial products, and reworked phytodetritus that form a longer-term sediment food
641 bank. This conclusion is also reflected by our findings where, as indicated by LDA and the

642 mixing model, microalgae contributed only a small amount to the bivalve diet (except *N.*
643 *radiata*). The reliance on bacterially reworked OM was even higher for DBO2, despite the fact
644 that the Chirikov Basin is characterized by high currents and higher inputs of fresh PP may be
645 expected (Grebmeier, et al., 2015a; Pisareva, et al., 2015). Similarly, higher reliance on
646 bacterially reworked OM was observed at Hanna Shoal (in comparison to DBO 4 and 5), which,
647 although the most northern location, was sampled later in the year (August). However, as both *M.*
648 *calcarea* and *E. tenuis* are deposit feeders it is likely that they were mainly utilizing deposited
649 sedimentary OM, and thus already highly reworked by bacteria, and in that case, they did not
650 have access to fresh suspended OM.

651 Interestingly, in the DBO3 area, where PP is very high, currents slow down and phytodetritus
652 is exported rapidly to the benthos (Grebmeier, et al., 2015a) deposit feeding bivalves displayed
653 similar $\delta^{13}C_{AA}$ patterns as further south while suspension feeders showed a higher proportion of
654 microalgae contributions (Table 2; Fig. 6). The fingerprinting approach showed that surface
655 deposit (*M. calcarea*) and subsurface deposit feeders (*E. tenuis, N. pernula*) utilized bacterial
656 (detrital) and microalgae in similar proportions while suspension feeders (*M. arenaria, S.*
657 *groenlandicus*) used more fresh OM, but nevertheless bacteria dominated in the diet. Although
658 more data are needed for conclusive determinations, these results suggest that the high fresh
659 phytoplankton biomass in the water column was only partially available for the suspension and
660 surface deposit feeding bivalves, which instead used more reworked detritus material and most
661 likely advective, more reworked carbon from the south than *in situ* new PP.

662

663 *4.3. Conclusions: CSIA-AA analysis challenges*

664

665 It is well documented that the stable isotope analysis of bulk organic materials is suitable to
666 detect longer-term (weeks to months) diet (e.g. Hobson and Welch, 1992; Layman, et al., 2012).
667 Studies conducted on deep-sea corals integrating information over the long (years) scales (Schiff,
668 et al., 2014; McMahon, et al., 2018) confirm that the figerprinting method and use of AAs can be
669 applied successfully. However, for CSIA-AA analysis to be most useful, the turnover time of
670 AAs is crucial to correctly assess food sources of benthic fauna. Studies on AA turnover remain
671 scarce, although some recent work has documented very long turnover times, up to thousands of
672 years, in deep marine sediments due to low metabolic rates of organisms and bacteria (Lomstein,
673 et al., 2012; Braun, et al., 2017; Møller, et al., 2018). Studies conducted in more productive
674 shallow sediments, however, suggest that AA turnover time is more likely in the range of weeks
675 to one year (Lomstein, et al., 1989; Arndt, et al., 2013), depending on the specific synthetic
676 pathways of the particular AA, the life stage of the organism and the organisms itself (O'Brien, et
677 al., 2002; Arndt, et al., 2013). Some AAs have very fast turnover times, especially non-essential
678 AAs, while others remain unchanged much longer. Also, the turnover time can change seasonally
679 and is faster during the winter in bivalves from temperate areas (Hawkins, 1985; 1991). However,
680 the essential AAs can be re-used by temperate marine mussels, which facilitates their longer
681 turnover time (Hawkins, 1991). This may present a challenge for highly seasonal ecosystems at
682 high latitudes. For example, if turnover times of essential AAs in the studied bivalves greatly
683 exceeded the period of PP, the fingerprinting technique used will not be able to fully identify a
684 clear preference for fresh PP, even if a bivalve fed exclusively on fresh OM while it was
685 available. It is therefore difficult to conclude if a mixed diet (e.g. *S. groenlandicus* at DBO3)
686 indicates an overall mixed diet over a longer period or a complete dietary switch during a short
687 food pulse of fresh PP. The time between the arrival of spring bloom production to the sea floor,
688 and our sampling might be too short an interval for the $\delta^{13}C_{AA}$ data to be sensitive to it although

689 our results do not suggest that. Studies on AA turnover times are critical to correctly assess the
690 time between the changes in the diet and changes in the $\delta^{13}C_{AA}$ value of different AAs, as well
691 changes to the AAs through space and time, particularly in the marine sediments. This issue is
692 particularly crucial for studies in highly seasonal ecosystems.

693 Overall, the $\delta^{13}C_{AA}$ patterns were shown to be a useful technique for food source
694 determination. Compared to bulk data analysis CSIA-AA allows for the inclusion of more
695 potential carbon sources and is not affected by the variable trophic fraction (depending on source,
696 consumer species, trophic level). However, there are still some challenges. Chemical signatures
697 of essential and non-essential AAs have been reported to be highly conservative among broad
698 taxonomic groups and not to vary significantly by location (Larsen, et al 2009, 2013, 2015).
699 Larsen, et al., (2013) showed that individual AAs $\delta^{13}C$ patterns have a large potential to
700 distinguish between organic carbon derived from algae, seagrass, terrestrial plants, bacteria and
701 fungi, and later, that sedimentary diagenesis may lead to an increased contribution of bacterial
702 sources over time (Larsen, et al., 2015). However, most prior studies were undertaken as
703 controlled feeding experiments or cultures, which simplifies many challenges that occur in the
704 natural environment. That is particularly true for the ecosystems where multiple food sources are
705 present and species are able to feed on OM that can be a mixture of many primary producers and,
706 in addition, is often highly reworked by microbial activity. If the mixture of ice algal,
707 phytoplankton and bacterial production, in the form of detritus both in the sediment and as
708 resuspended material, is the main food source, the identification of a specific food source is
709 challenging and requires additional information on source $\delta^{13}C_{AA}$ (Rowe et al., 2019). The
710 application of CSIA-AA for carbon isotopes is not always straightforward, and without baseline
711 and prey data, the determination of whether essential AAs are isotopically fractionated or not
712 relative to their diet may not always be possible. Expanding the existing data base (Larsen, et al.,

2013) of source $\delta^{13}C_{AA}$ is important, particularly from natural ecosystems (Whiteman, et al., 2019) and with marine microalgae including both phytoplankton and sea-ice algae. More information on marine fungi and bacteria is also needed as some decomposers (fungi and bacteria) included in the Larsen, et al. (2013) source data are of terrestrial origin. Further, combining $\delta^{13}C$ CSIA-AA with analysis of other biomarkers, such as highly-branched isoprenoids (e.g. Koch, et al., 2020) might be helpful in investigating differences among bacterially re-worked OM, phytoplankton and ice algae.

We have presented one of the first $\delta^{13}C$ CSIA-AA analysis for benthic fauna and potential food sources for dominant bivalve species on the Pacific Arctic shelf. Patterns of $\delta^{13}C_{AA}$ values in this study revealed useful information for assessing animal feeding behavior, OM sources use and thus, ecosystem functioning, even if not all of the patterns were clear and unambiguous. Our data indicated that bivalves fed mainly on a mixture of bacteria and microalgae in different proportions depending upon species identity and, to less extend, sampled locations, largely following our initial hypothesis that the share of fresh PP in bivalves' diet will increase as a northward gradient. We recommend further studies on the application of CSIA-AA, and $\delta^{13}C_{AA}$ determinations in seasonal marine environments and where animal diets are known to consist of mixed sources.

5. Acknowledgements

This work was conducted within the framework of the Distributed Biological Observatory program (US National Science Foundation award 1204082, 1702137 and 1917434 to J. Grebmeier and L. Cooper) and was further supported by Polish National Science Centre grant no.

DEC-2013/08/M/NZ8/00592 to M. Kędra. Additional financial support for the efforts of M. Zhang, D. Biasatti, L. Cooper, and J.M. Grebmeier was provided by the US Bureau of Ocean Energy Management, Alaska Outer Continental Shelf Region, Anchorage, Alaska under BOEM Cooperative Agreement No. M11AC00007 as part of the Chukchi Sea Offshore Monitoring in Drilling Area (COMIDA). M. Zhang was additionally supported by a North Pacific Research Board Graduate Fellowship. We thank two anonymous reviewers whose comments greatly improved this manuscript.

References

1. Ambrose Jr., W.G., Clough, L.M., Tilney, P.R., Beer, L., 2001. Role of echinoderms in benthic remineralization in the Chukchi Sea. Marine Biol. 139, 937-947. Doi: 10.1007/s002270100652
2. Ambrose Jr., W.G., Renaud, P.E., 1997. Does a pulsed food supply to the benthos affect polychaete recruitment patterns in the Northeast Water Polynya? J. Mar. Syst. 10, 483-495. Doi: 10.1016/S0924-7963(96)00053-X
3. Ardyna, M., Arrigo, K.R., 2020. Phytoplankton dynamics in a changing Arctic Ocean. Nat. Clim. Chang. 10, 892–903. Doi: 10.1038/s41558-020-0905-y
4. Arndt, S., Jørgensen, B.b., LaRowe, D.E., Middelburg, J.J., Pancost, R.D., Regnier, P., 2013. Quantifying the degradation of organic matter in marine sediments: A review and synthesis. Earth-Sci. Rev. 123, 53-86. Doi: 10.1016/j.earscirev.2013.02.008
5. Arrigo, K.R., van Dijken, G., 2011. Secular trends in Arctic Ocean net primary production. J. Geophys. Res. 116, C09011. Doi:10.1029/2011JC007151.

6. Arrigo, K.R., van Dijken, G.L., 2015. Continued increases in Arctic Ocean primary production. Progr. Oceanogr. 136, 60-70. Doi: 10.1016/j.pocean.2015.05.002

7. Arthur, K.E., Kelez, S., Larsen, T., Choy, C.A., Popp, B.N., 2014. Tracing the biosynthetic source of essential amino acids in marine turtles using $\delta^{13}C$ fingerprints. Ecology 95, 1285-1293 Doi: 10.1890/13-0263.1

8. Assmy, P., Fernandez-Mendez, M., Duarte, P., Meyer, A., Randelhoff, A., Mundy, C.J., Olsen, L.M., Kauko, H.M., Bailey, A., Chierici, M., Cohen, L., Doulgeris, A.P., Ehn, J.K., Fransson, A., Gerland, S., Hop, H., Hudson, S.R., Hughes, N., Itkin, P., Johnsen, G., King, J.A., Koch, B.P., Koenig, Z., Kwasniewski, S., Laney, S.R., Nicolaus, M., Pavlov, A.K., Polashenski, C.M., Provost, C., Rosel, A., Sandbu, M., Spreen, G., Smedsrud, L.H., Sundfjord, A., Taskjelle, T., Tatarek, A., Wiktor, J., Wagner, P.M., Wold, A., Steen, H., Granskog, M.A., 2017. Leads in Arctic pack ice enable early phytoplankton blooms below snow-covered sea ice. Sci. Rep. 7, 40850. Doi: 10.1038/srep40850

9. Braun, S., Mhatre, S.S., Jaussi, M., Røy, H., Kjeldsen, K.U., Pearce, C., Seidenkrantz, M.S., Jørgensen, B.B., Lomstein, B.Aa., 2017. Microbial turnover times in the deep seabed studied by amino acid racemization modelling. Scientific Rep. 7, 5680. Doi:10.1038/s41598-017-05972-z

10. Chikaraishi, Y., Ogawa, N.O., Kashiyama, Y., Takano, Y., Suga, H., Tomitani, A., Miyashita, H., Kitazato, H., Ohkouchi, N., 2009. Determination of aquatic food-web structure based on compound-specific nitrogen isotopic composition of amino acids. Limnol. Oceanogr. Methods*,* 7*,* 740-750. Doi:10.4319/lom.2009.7.740.

11. Chikaraishi, Y., Steffan, S.A., Ogawa, N.O., Ishikawa, N.F., Sasaki, Y., Tsuchiya, M., Ohkouchi, N., 2014. High-resolution food webs based on nitrogen isotopic composition of amino acids. Ecol. Evol. 4, 2423-2449. Doi: 10.1002/ece3.1103

782 12. Clarke, K.R., Gorley, R.N. 2015. Getting started with PRIMER v7 PRIMER-E:
783 Plymouth.
784 13. Comiso, J.C., 2012. Large decadal decline of the arctic multiyear ice cover. J. Clim. 25,
785 1176-1193. Doi: 10.1175/JCLI-D-11-00113.1
786 14. Cooper, L.W., Grebmeier, J.M., Larsen, I.L., Egorov, V.G., Theodorakis, C., Kelly, H.P.,
787 Lovvorn, J.R., 2002. Seasonal variation in sedimentation of organic materials in the St.
788 Lawrence Island polynya region, Bering Sea. Marine Ecology Progress Series 226, 13-26.
789 Doi: 10.3354/meps226013

790 15. Cooper, L.W., Larsen, I.L., Grebmeier, J.M., Moran, S.B., 2005. Detection of rapid
791 deposition of sea ice-rafted material to the Arctic Ocean benthos using the cosmogenic tracer
792 ^{7}Be. Deep Sea Res. II 52, 3452-3461. Doi: 10.1016/j.dsr2.2005.10.011
793 16. Cooper, L.W., Sexson, M.G., Grebmeier, J.M., Gradinger, R., Mordy, C.W., Lovvorn,
794 J.R. 2013. Linkages between sea ice coverage, pelagic-benthic coupling and the distribution of
795 spectacled eiders: observations in March 2008, 2009 and 2010 from the northern Bering Sea.
796 Deep Sea Res. II 94, 31-43. Doi: 10.1016/j.dsr2.2013.03.009

797 17. Cooper, L.W., Grebmeier, J.M., 2018. Deposition patterns on the Chukchi shelf using
798 radionuclide inventories in relation to surface sediment characteristics. Deep Sea Research
799 Part II: Topical Studies in Oceanography 152, 48-66. Doi: 10.1016/j.dsr2.2018.01.009

800 18. Divine, L.M., Bluhm, B., Mueter, F., Iken, K., 2017. Diet analysis of Alaska Arctic snow
801 crabs (*Chionoecetes opilio*) using stomach contents and δ^{13}C and δ^{15}N stable isotopes. Deep
802 Sea Res. II 135, 124-136. Doi: 10.1016/j.dsr2.2015.11.009

803 19. Docherty, G., Jones, V., Evershed, R.P., 2001. Practical and theoretical considerations in the
804 gas chromatography/ combustion/isotope ratio mass spectrometry $\delta^{13}C$ analysis of small
805 polyfunctional compounds. Rapid Commun. in Mass Spectrom. 15, 730–738. Doi:
806 10.1002/rcm.270
807 20. Elliott Smith, E.A., Harrod, C., Newsome, S.D., 2018. The importance of kelp to an intertidal
808 ecosystem varies by trophic level: insights from amino acid $\delta^{13}C$ analysis. Ecosphere 9,
809 e02516. Doi: 10.1002/ecs2.2516
810 21. Feder, H.M., Iken, K., Blanchard, A.L., Jewett, S.C., Schonberg, S., 2011. Benthic food
811 web structure in the southerneastern Chukchi Sea: an assessment using $\delta^{13}C$ and $\delta^{15}N$
812 analyses. Polar Biol. 34: 521-532. Doi: 10.1007/s00300-010-0906-9
813 22. Frey, K.E., Maslanik, J.A., Clement Kinney, J., Maslowski, W., 2014. Recent variability
814 in sea ice cover, age, and thickness in the Pacific Arctic Region, in: Grebmeier, J.M.,
815 Maslowski, W. (Eds.), The Pacific Arctic Region: Ecosystem status and trends in a rapidly
816 changing environment. Springer, Dordrecht, pp. 31–63
817 23. Frey, K.E., Moore, G.W.K., Cooper, L.W., Grebmeier, J.M., 2015. Divergent patterns of
818 recent sea ice cover across the Bering, Chukchi and Beaufort seas of the Pacific Arctic
819 Region. Progr. Oceanogr. 136, 32-49. Doi: 10.1016/j.pocean.2015.05.009
820 24. Frey, K.E., Comiso, J.C., Cooper, L.W., Grebmeier, J.M., Stock, L.V., 2018. Arctic
821 Ocean primar productivity: The response of marine algae to climate warming and sea ice
822 decline. Arctic Report Card, http://www.arctic.noaa.gov/reportcard.
823 25. Fetterer, F., Knowles, K., Meier, W.N., Savoie, M., Windnagel, A.K., 2017. Sea Ice Index,
824 Version 3, updated daily. Subset used: Boulder, Colorado USA. NSIDC: National Snow and
825 Ice Data Center. doi: https://doi.org/10.7265/N5K072F8. [Date Accessed: 11.03.2021].

826 26. Goethel, C.L., Grebmeier, J.M., Cooper, L.W., 2019. Changes in abundance and biomass of
827 the bivalve *Macoma calcarea* in the northern Bering Sea and the southeastern Chukchi Sea
828 from 1998 to 2014, tracked through dynamic factor analysis models. Deep Sea Res. II 162,
829 127-136. Doi: 10.1016/j.dsr2.2018.10.007
830 27. Grebmeier, J.M., 2012. Shifting patterns of life in the Pacific Arctic and sub-arctic seas.
831 Ann. Rev. Mar. Sci. 4, 63-78. Doi: 10.1146/annurev-marine-120710-100926
832 28. Grebmeier, J.M., Barry, J.P., 2007. Benthic processes in polynyas, in: Smith Jr, W.O.,
833 Barber, D.G. (Eds.), Polynyas: Windows to the World. Elsevier Oceanogr. Ser., Amsterdam:
834 Elsevier, pp. 363-390.
835 29. Grebmeier, J.M., Cooper, L.W., 1995. Influence of the St. Lawrence Island polynya on
836 the Bering Sea benthos. J. Geophys. Res. 100, 4439-4460. Doi: 10.1029/94JC02198
837 30. Grebmeier, J.M., Cooper, L.W., 2014. PacMARS Surface Sediment Parameters, Version
838 1.0. http://dx.doi.org/10.5065/D6416V3G.
839 31. Grebmeier, J.M., Cooper, L.W., Feder, H.M., Sirenko, B.I., 2006. Ecosystem dynamics of
840 the Pacific-influenced Northern Bering and Chukchi Seas in the Amerasian Arctic. Progr.
841 Oceanogr. 71, 331-361. Doi: 10.1016/j.pocean.2006.10.001
842 32. Grebmeier, J.M., Moore, S.E., Overland, J.E., Frey, K.E., Gradinger, R., 2010. Biological
843 response to recent Pacific Arctic sea ice retreats. Eos Transactions American Geophys. Union
844 91, 161–162. Doi: 10.1029/2010EO180001
845 33. Grebmeier, J.M., Bluhm, B.A., Cooper, L.W., Danielson, S., Arrigo, K.R., Blanchard,
846 A.L., Clarke, J.T., Day, R.H., Frey, K.E., Gradinger, R.R., Kędra, M., Konar, B., Kuletz, K.J.,
847 Lee, S.H., Lovvorn, J.R., Norcross, B.L., Okkonen, S.R., 2015a. Ecosystem characteristics and
848 processes facilitating persistent macrobenthic biomass hotspots and associated benthivory in
849 the Pacific Arctic. Progr. Oceanogr. 136, 92-114. Doi: 10.1016/j.pocean.2015.05.006

850 34. Grebmeier, J.M., Bluhm, B.A., Cooper, L.W., Denisenko, S.G., Iken, K., Kędra, M.,
851 Serratos, C., 2015b. Time-series benthic community composition and biomass and associated
852 environmental characteristics in the Chukchi Sea during the RUSALCA 2004-2012 Program.
853 Oceanography 28, 116-133. Doi: 10.5670/oceanog.2015.61
854 35. Grebmeier, J.M, Cooper, L.W., 2016. The Saint Lawrence Island Polynya: A 25-Year
855 Evaluation of an Analogue for Climate Change in Polar Regions. In: Glibert, P.M., Kana,
856 T.M. (Eds.), Aquatic Microbial Ecology and Biogeochemistry: A Dual Perspective. Springer,
857 Cham. DOI 10.1007/978-3-319-30259-1_14
858 36. Grebmeier, J.M., Frey, K.E., Cooper, L.W., Kędra, M, 2018. Trends in Benthic
859 Macrofaunal Populations, Seasonal Sea Ice Persistence, and Bottom Water Temperatures in
860 the Bering Strait Region. Oceanography 31: 136-151. Doi: 10.5670/oceanog.2018.224
861 37. Hawkins, A.J.S., 1985. Relationships between the synthesis and breakdown of protein,
862 dietary absorption and turnovers of nitrogen and carbon in the blue mussel, *Mytilus edulis* L.
863 Oecologia 66, 42-49. Doi: 10.1007/BF00378550Hawkins, A.J.S., 1991. Protein turnover: a
864 functional appraisal. Functional Ecol. 5, 222-233. Doi: 10.2307/2389260
865 38. Hill, V., Ardyna, M., Lee, S.H., Varela, D.E., 2018. Decadal trends in phytoplankton
866 production in the Pacific Arctic Region from 1950 to 2012. Deep Sea Res. II. 152, 82-94. Doi:
867 10.1016/j.dsr1012.2016.1012.1015
868 39. Hirawake, T., Shinmyo, K., Fujiwara, A., Saitoh, S., 2012. Satellite remote sensing of
869 primary productivity in the Bering and Chukchi Seas using an absorption-based approach.
870 ICES J. Mar. Sci. 69, 1194-1204. Doi: 10.1093/icesjms/fss111
871 40. Hobson, K.A., Welch, H.E., 1992. Determination of trophic relationships within a high
872 Arctic marine food web using $\delta^{13}C$ and $\delta^{15}N$ analysis. Mar. Ecol. Progr. Ser. 84, 9-18. Doi:
873 10.1360/04wd0283

874 41. Howland, M.R., Corr, L.T., Young, S.M.M., Jones, V., Jim, S., Van Der Merwe, N.J.,
875 Mitchell, A.D., Evershed, R.P., 2003. Expression of the dietary isotope signal in the
876 compound-specific $\delta^{13}C$ values of pig bone lipids and amino acids. Int. J. Osteoarchaeol. 13,
877 54-65. Doi: doi.org/10.1002/oa.658
878 42. Iken, K., Bluhm, B.A., Gradinger, R., 2005. Food web structure in the high Arctic Canada
879 basin: evidence from $\delta^{13}C$ and $\delta^{15}N$ analysis. Polar Biol. 28, 238-249. Doi: 10.1007/s00300-
880 004-0669-2
881 43. Iken, K., Bluhm, B., Dunton, K., 2010. Benthic food-web structure under differing water
882 mass properties in the southern Chukchi Sea. Deep Sea Res. II 57, 71-85. Doi:
883 10.1016/j.dsr2.2009.08.007
884 44. IPCC, 2019., IPCC Special Report on the Ocean and Cryosphere in a Changing Climate
885 [Pörtner, H.-O., Roberts, D.C., Masson-Delmotte, V., Zhai, P., Tignor, M., Poloczanska, E.
886 Mintenbeck, K., Alegría, A., Nicolai, M., Okem, A., Petzold, J., Rama, B., Weyer, N.M.
887 (eds.)]. In press.
888 45. Keil, R.G., Fogel, M.L., 2001. Reworking of amino acid in marine sediments: Stable carbon
889 isotopic composition of amino acids in sediments along the Washington coast. Limnol.
890 Oceanogr. 46, 14-23. Doi: 10.4319/lo.2001.46.1.0014
891 46. Kędra, M., Kuliński, K., Walkusz, W., Legeżyńska, J., 2012. The shallow benthic food
892 web structure in the high Arctic does not follow seasonal changes in the surrounding
893 environment. Estuar. Coast. Shelf Sci. 114, 183-191. Doi:10.1016/j.ecss.2012.1008.1015.
894 47. Kędra, M., Moritz, C., Choy, E.S., David, C., Degen, R., Duerksen, S., Ellingsen, I.,
895 Górska, B., Grebmeier, J.M., Kirievskaya, D., van Oevelen, D., Piwosz, K., Samuelsen, A.,
896 J.M., W., 2015. Status and trends in the structure of Arctic benthic food webs. Polar Research
897 34, 23775. Doi: 10.3402/polar.v34.23775

898 48. Kędra, M., Cooper, L.W., Zhang, M., Biasatti, D., Grebmeier, J.M., 2019, Benthic trophic
899 sensitivity to on-going changes in Pacific Arctic seasonal sea ice cover – insights from the
900 nitrogen isotopic composition of amino acids. Deep Sea Res. II 162, 137-151. Doi:
901 10.1016/j.dsr2.2019.01.002
902 49. Koch, C.W., Cooper, L.W., Grebmeier, J.M., Frey, K., Brown, T.A., 2020. Ice algae resource
903 utilization by benthic macro- and megafaunal communities on the Pacific Arctic shelf
904 determined through lipid biomarker analysis. Mar Ecol Prog Ser 651, 23-43. Doi:
905 10.3354/meps13476
906 50. Kwok, R., Rothrock, D.A., 2009. Decline in Arctic sea ice thickness from submarine and
907 ICESat records: 1958-2008. Geophys. Res. Lett. 36, L15501. Doi: 10.1029/2009GL039035
908 51. Lalande, C., Grebmeier, J.M., Wassmann, P., Cooper, L.W., Flint, M.V., Sergeeva, V.M.,
909 2007. Export fluxes of biogenic matter in the presence and absence of seasonal sea ice cover
910 in the Chukchi Sea. Cont. Shelf Res. 27, 2051-2065. Doi: 10.1016/j.csr.2007.05.005
911 52. Lalande, C., Grebmeier, J.M., Hopcroft, R.R., Danielson, S.L., 2020. Annual cycle of export
912 fluxes of biogenic matter near Hanna Shoal in the northeast Chukchi Sea. Deep Sea Res. II
913 177, 104730. Doi: 10.1016/j.dsr2.2020.104730
914 53. Larsen, T., Taylor, D.L., Leigh, M.B., O'Brien, D.M., 2009. Stable isotope fingerprinting:
915 a novel method for identifying plant, fungal, or bacterial origins of amino acids. Ecology 90,
916 3526-3535. Doi: 10.1890/08-1695.1
917 54. Larsen, T., Wooller, M.J., Fogel, M.L., O'Brien, D.M., 2012. Can Amino Acid Carbon
918 Isotope Ratios Distinguish Primary Producers in a Mangrove Ecosystem? Rapid Commun.
919 Mass Spectrom. 26, 1541-1548. Doi: 10.1002/rcm.6259

920 55. Larsen, T., Ventura, M., Andersen, N., O'Brien, D.M., Piatowski, U., McCarthy, M.D.,
921 2013. Tracing carbon sources through aquatic and terrestrial food webs using amino acid
922 stable isotope fingerprinting. PLoS ONE 8, e73441. Doi:10.1371/journal.pone.0073441
923 56. Larsen, T., Bach, L.T., Salvatteci, R., Wang, Y.V., Andersen, N., Ventura, M., McCarthy,
924 M.D., 2015. Assessing the potential of amino acid $\delta^{13}C$ patterns as a carbon source tracer in
925 marine sediments: effects of algal growth conditions and sedimentary diagenesis.
926 Biogeosciences 12, 1613-1651. Doi: 10.5194/bg-12-4979-2015
927 57. Layman, C.A., Araujo, M.S., Boucek, R., Hammerschlag-Peyer, C.M., Harrison, E., Jud,
928 Z.R., Matich, P., Rosenblatt, A.E., Vaudo, J.J., Yeager, L.A., Post, D.M., Bearhop, S., 2012.
929 Applying stable isotopes to examine food-web structure: an overview of analytical tools. Biol.
930 Rev. 87, 545-562. Doi: 10.1111/j.1469-185X.2011.00208.x
931 58. Lee, S.H., Hyoung, M.J., Yun, M.S., Whitledge, T.E., 2012. Recent phytoplankton
932 productivity of the northern Bering Sea during early summer in 2007. Polar Biol. 35, 83-98.
933 Doi: 10.1007/s00300-011-1035-9
934 59. Lomstein, B.A., Blackburn, T.H., Henriksen, K., 1989. Aspects of nitrogen and carbon
935 cycling in the northern Bering Shelf sediment. I. The significance of urea turnover in the
936 mineralization of NH_4^+. Mar. Ecol. Progr. Ser. 57, 237-247. Doi: 10.3354/meps057237
937 60. Lomstein, B.A., Langerhuus, A.T. D'Hondt, S.D., Jørgensen, B.B., Spivack, A.J., 2012.
938 Endospore abundance, microbial growth and necromass turnover in deep sub-seafloor
939 sediment. Nature 484, 101-104. Doi: 10.1038/nature10905
940 61. Lorrain, A., Graham, B., Menard, F., Popp, B., Bouillon, S., van Breugel, P., Cherel, Y.,
941 2009. Nitrogen and carbon isotope values of individual amino acids: a tool to study foraging
942 ecology of penguins in the Southern Ocean. Mar. Ecol. Progr. Ser. 391, 293-306.
943 Doi:10.3354/meps08215

944 62. Lovvorn, J.R., Richman, S.E., Grebmeier, J.M., 2003. Diet and body condition of
945 spectacled eiders wintering in pack ice of the Bering Sea. Polar Biol. 26, 259-267. Doi:
946 10.1007/s00300-003-0477-0
947 63. Lovvorn, J.R., Cooper, L.W., Brooks, M.L., DeRuyck, C.C., Bump, J.K., Grebmeier,
948 J.M., 2005. Organic matter pathways to zooplankton and benthos under pack ice in late winter
949 and open water in late summer in the north-central Bering Sea. Mar. Ecol. Progr. Ser. 291,
950 135-150. Doi: 10.3354/meps291135
951 64. Lowry, K.E., Pickart, R.S., Mills, M.M., Brown, Z.W., Van Dijken, G., Bates, N.R.,
952 Arrigo, K.R., 2015. The influence of winterwater on phytoplankton blooms in the Chukchi
953 Sea. Deep Sea Res. II 118, 53-72. Doi: 10.1016/j.dsr2.2015.06.006
954 65. Macko, S., Uhle, M.E., 1997. Stable nitrogen isotope analysis of amino acid enantiomers
955 by gas chromatography/combustion/isotope ratio mass spectrometry. Anal. Chem. 69, 926-
956 929. Doi: 10.1021/ac960956l
957 66. McCarthy, M.D., Benner, R., Lee, C., Hedges, J.I., Fogel, M.L., 2004. Amino acid carbon
958 isotopic fractionation patterns in oceanic dissolved organic matter: an unaltered
959 photoautotrophic source for dissolved organic nitrogen in the ocean? Mar. Chem. 92, 123-134.
960 Doi: 10.1016/j.marchem.2004.06.021
961 67. McCarthy, M.D., Benner, R., Lee, C., Fogel, M.L., 2007. Amino acid nitrogen isotopic
962 fractionation patterns as indicators of heterotrophy in plankton, particulate, and dissolved
963 organic matter. Geochim. Cosmochim. Acta 71, 4727-2744. Doi: 10.1016/j.gca.2007.06.061
964 68. McClelland, J.W., Montoya, J.P., 2002. Trophic relationships and the nitrogen isotopic
965 composition of amino acids in plankton. Ecology 83, 2173-2180. Doi: 10.1890/0012-
966 9658(2002)083[2173:TRATNI]2.0.CO;2

967 69. McGovern, M., Berge, J., Szymczycha, B., Węsławski, J.M., Renaud, P.E. 2018.
968 Hyperbenthic food-web structure in an Arctic fjord. Mar. Ecol. Prog. Ser. 603, 29-46. Doi:
969 10.3354/meps12713
970 70. McMahon, K., Thorrold, S.R., Houghton, L.A., Berumen, M.L., 2016. Tracing carbon
971 flow through coral reef food webs using a compound specific stable isotope approach.
972 Oecologia 180, 809-821. Doi: 10.1007/s00442-015-3475-3
973 71. McMahon, K.W., Fogel, M.L., Elsdon, T., Thorrold, S.R., 2010. Carbon isotope
974 fractionation of amino acids in fish muscle reflects biosynthesis and isotopic routing from
975 dietary protein. J. Animal Ecol. 79, 1132-1141. Doi: 10.1111/j.1365-2656.2010.01722.x
976 72. McMahon, K.W., Hamady, L.L., Thorrold, S.R., 2013. Ocean Ecogeochemistry: A
977 Review. Oceanogr. Mar. Biol. 51, 327-374.
978 73. McMahon, K.W., Polito, M.J., Abel, S., McCarthy, M.D., Thorrold, S.R., 2015. Carbon
979 and nitrogen isotope fractionation of amino acids in an avian marine predator, the gentoo
980 penguin (*Pygoscelis papua*). Ecol. Evol. 5, 1278-1290. Doi: 10.1002/ece3.1437
981 74. McMahon, K.W., Williams, B., Guilderson, T.P., Glynn, D.S., McCarthy, M.D., 2018.
982 Calibrating amino acid $\delta^{13}C$ and $\delta^{15}N$ offsets between polyp and protein skeleton to develop
983 proteinaceous deep-sea corals as paleoceanographic archives. Geochim. Cosmochim. Acta
984 220, 261-275. Doi: 10.1016/j.gca.2017.09.048
985 75. McTigue, N.D., Dunton, K.H., 2014. Trophodynamics and organic matter assimilation
986 pathways in the northeast Chukchi Sea, Alaska. Deep Sea Res. II 102, 84-96. Doi:
987 10.1016/j.dsr2.2013.07.016
988 76. McTigue, N.D., Bucolo, P., Liu, Z., Dunton, K.H., 2015. Pelagic-benthic coupling, food
989 webs, and organic matter degradation in the Chukchi Sea: Insights from sedimentary pigments
990 and stable carbon isotopes. Limnol. Oceanogr. 60, 429-445. Doi: 10.1002/lno.10038

991 77. Meier, W.N., 2017. Losing Arctic sea ice: observations of the recent decline and the long-
992 term context. in: Thomas, D.N., (Ed.), Sea Ice. Jon Wiley & Sons, Ltd, Chichester, UK. Doi:
993 10.1002/9781118778371.ch11
994 78. Mohan, S.D., Connelly, T.L., Harris, C.M., Dunton, K.H., McClelland, J.W., 2016. Seasonal
995 trophic linkages in Arctic marine invertebrates assessed via fatty acids and compound-
996 specific
997 79. stable isotopes. Ecosphere 7(8):e01429. Doi: 10.1002/ecs2.1429
998 80. Møller, M.H., Glombitza, C., Lever, M.A., Deng, L., Morono, Y., Inagaki, F., Doll, M.,
999 Su, C.C. Lomstein, B.A., 2018. D:L-amino acid modeling reveals fast microbial turnover of
1000 days to months in the subsurface hydrothermal sediment of Guaymas Basin. Frontiers in
1001 Microbiol. 9: 967-967. Doi: 10.3389/fmicb.2018.00967
1002 81. Moore, S.E., Grebmeier, J.M., 2018. The Distributed Biological Observatory: Linking
1003 physics to biology in the Pacific Arctic Region. Arctic 71, 1-7. Doi: 10.14430/arctic4606
1004 82. Moore, S.E., Stabeno, P.J., 2015. Synthesis of Arctic Research (SOAR) in marine
1005 ecosystems of the Pacific Arctic. Progr. Oceanogr. 136, 1-11. Doi:
1006 10.1016/j.pocean.2015.05.017
1007 83. Moore, S.E., Kuletz, K.J., 2018. Marine birds and mammals as ecosystem sentinels in and
1008 near Distributed Biological Observatory regions: An abbreviated review of published accounts
1009 and recommendations for integration to ocean observatories. Deep Sea Res. II. Doi:
1010 10.1016/j.dsr2.2018.09.004
1011 84. Moran, S.B., Kelly, R.P., Hagstrom, K., Smith, J.N., Grebmeier, J.M., Cooper, L.W., Cota,
1012 G., Walsh, J.J., Bates, N.R., Hansell, D.A., Maslowski, W., Nelson, R.P., Mulsow, S., 2005.
1013 Seasonal changes in POC export flux in the Chukchi Sea and implications for water column-

benthic coupling in Arctic shelves. Deep Sea Res. II 52, 3427-3451. Doi: 10.1016/j.dsr2.2005.09.011

85. Morata, N., Michaud, E., Włodarska-Kowalczuk, M., 2015. Impact of early food input on the Arctic benthos activities during the polar night. Polar Biol. 38, 99-114. Doi: 10.1007/s00300-013-1414-5

86. Morata, N., Michaud, E., Poullaouec, M.-A., Devesa, J., Le Goff, M., Corvaisier, R., Renaud, P.E., 2020. Climate change and diminishing seasonality in Arctic benthic processes. Phil. Trans. R. Soc. A.37820190369. Doi: 10.1098/rsta.2019.0369

87. Mundy, C.J., Gosselin, M., Gratton, Y., Brown, K., Galindo, V., Campbell, K., Lecasseur, M., Barber, D., Papakyriakou, T., Belanger, S., 2014. Role of environmental factors on phytoplankton bloom initiation under landfast sea ice in Resolute Passage. Canada. Mar. Ecol. Progr. Ser. 497, 39-49. Doi: 10.3354/meps10587

88. Nielsen, J.M., Popp, B.N., Winder, M., 2015. Meta-analysis of amino acid stable nitrogen isotope ratios for estimating trophic position in marine organisms. Oecologia 178, 631-642. Doi: 10.1007/s00442-015-3305-7

89. North, C.A., Lovvorn, J.R., Kolts, J.M., Brooks, M.L., Cooper, L.W., Grebmeier, J.M., 2014. Deposit-feeder diets in the Bering Sea: potential effects of climatic loss of sea ice-related microalgal blooms. Ecol. Appl. 24, 1525-1542 Doi:10.1890/13-0486.1

90. O'Brien, D.M., Fogel, M.L., Boggs, C.L., 2002. Renewable and nonrenewable resources: Amino acid turnover and allocation to reproduction in Lepidoptera. Proc. Natl. Acad. Sci. USA 99, 4413-4418. Doi: 10.1073/pnas.072346699

91. Parkinson, C.L., Comiso, J.C., 2013. On the 2012 record low Arctic sea ice cover: Combined impact of preconditioning and an August storm. Geophys. Res. Lett. 40, 1356–1361. Doi: 10.1002/grl.50349

1038 92. Parnell, A.C., Inger, R., Bearhop, S., Jackson, A.L., 2010. Source partitioning using stable
1039 isotopes: coping with too much variation. Plos ONE 5(3), e9672. Doi:
1040 10.1371/journal.pone.0009672
1041 93. Petrenko, D., Pozdnyakov, D., Johannessen, J., Counillon, F., Sychov, V., 2013. Satellite-
1042 derived multi-year trend in primary production in the Arctic Ocean. Int. J. Remote Sens. 34,
1043 3903-3937. Doi: 10.1080/01431161.2012.762698
1044 94. Pisareva, M.N., Pickart, R.S., Iken, K., Ershova, E.A., Grebmeier, J.M., Cooper, L.W.,
1045 Bluhm, B.A., Nobre, C., Hopcroft, R.R., Hu, H., Wang, J., Ashjian, C.J., Kosobokova, K.N.,
1046 T.E., W., 2015. The relationship between patterns of benthic fauna and zooplankton in the
1047 Chukchi Sea and physical forcing. Oceanography 28, 68-83. Doi: 10.5670/oceanog.2015.58
1048 95. Polyakov, I.V., Walsh, J.E., Kwok, R., 2012. Recent changes of Arctic multiyear sea ice
1049 coverage and the likely causes. Bull. Amer. Meteorol. Soc. 93, 145-151. Doi: 10.1175/BAMS-
1050 D-11-00070.1
1051 96. Post, D.M. 2002. Using stable isotopes to estimate trophic position: models, methods, and
1052 assumptions. Ecology 83, 703-718.
1053 97. Reeds, P., 2000. Dispensable and indispensable amino acids for humans. J. Nutr. 130,
1054 1835S–1840S.
1055 98. Richman, S.E., Lovvorn, J., 2003. Effects of clam species dominance on nutrient and
1056 energy acquisition by spectacled eiders in the Bering Sea. Mar. Ecol. Progr. Ser. 261, 283-297.
1057 Doi: 10.3354/meps261283
1058 99. Roca-Martí, M., Puigcorbé, V., Rutgers van der Loeff, M. M., Katlein, C., Fernández-
1059 Méndez, M., Peeken, I., Masqué P., 2016. Carbon export fluxes and export efficiency in the
1060 central Arctic during the record sea-ice minimum in 2012: a joint 234Th/238U and ^{210}Po/^{210}Pb
1061 study, J. Geophys. Res. Oceans 121, 5030–5049. Doi: 10.1002/2016JC011816.

100. Rogers, M., Bare, R., Gray, A., Scott-Moelder, T., Heintz, R., 2019. Assessment of two feeds on survival, proximate composition, and amino acid carbon isotope discrimination in hatchery-reared Chinook salmon. Fisheries Res. 219, 105303. Doi: 10.1016/j.fishres.2019.06.001.

101. Rowe, A.G., Iken, K., Blanchard, A.L., O'Brien, D.M., Døving Osvik, R., Uradnikova, M., Wooller, M.J. 2019. Sources of primary production to Arctic bivalves identified using amino acid stable carbon isotope fingerprinting. Isot. Environ. Healt. S. 55, 366-384. Doi: 10.1080/10256016.2019.1620742

102. Sabadel, A.J.M., Woodward, E.M.S., Van Hale, R., Frew, R.D., 2016. Compound-specific isotope analysis of amino acids: A tool to unravel complex symbiotic trophic relationships. Food Webs 6, 9-18. Doi: 10.1016/j.fooweb.2015.12.003

103. Sabadel, A.J.M., Durante, L.M., Wing, S.R., 2020. Stable isotopes of amino acids from reef fishes uncover Suess and nitrogen enrichment effects on local ecosystems. Mar. Ecol. Progr. Ser. 647:149-160. Doi: 10.3354/meps13414

104. Schiff, J.T., Batista, F.C., Sherwood, O.A., Guilderson, T.P., Hill, T.M., Ravelo, A.C., McMahon, K.W., McCarthy, M.D., 2014. Compound specific amino acid $\delta^{13}C$ patterns in a deep-sea proteinaceous coral: Implications for reconstructing detailed $\delta^{13}C$ records of exported primary production. Mar. Chem. 166, 82-91. Doi: 10.1016/j.marchem.2014.09.008

105. Serreze, M.C., Meier, W.N., 2019. The Arctic's sea ice cover: trends, variability, predictability, and comparisons to the Antarctic. Ann. N.Y. Acad. Sci., 1436: 36-53. Doi: 10.1111/nyas.13856

106. Serreze, M.C., Crawford, A.D., Stroeve, J.C., Barret, A.P., Woodgate, R.A., 2016. Variability, trends, and predictability of seasonal sea ice retreat and advance in the Chukchi Sea. J. Geophys. Res. Oceans 121, 7308-7325. Doi: 10.1002/2016JC011977

1086 107. Sheffield, G., Grebmeier, J.M., 2009. Pacific walrus (*Odobenus rosmarusdivergens*):
1087 differential prey digestion and diet. Mar. Mammal Sci. 25, 761-777. Doi: 10.1111/j.1748-
1088 7692.2009.00316.x
1089 108. Silberberger, M.J., Koziorowska-Makuch, K., Kuliński, K., Kędra, M., 2021. Stable
1090 isotope mixing models are biased by the choice of sample preservation and pre-treatment:
1091 Implications for studies of aquatic food webs. Front. Mar. Sci. 7, 621978. Doi:
1092 10.3389/fmars.2020.621978
1093 109. Silfer, J.A., Engel, M.H., Macko, S.A., Jumeau, E.J., 1991. Stable carbon isotope analysis
1094 of amino-acid enantiomers by conventional isotope ratio mass spectrometry and combined
1095 gas-chromatography isotope ratio mass-spectrometry. Anal. Chem. 63, 370-374. Doi:
1096 10.1021/ac00004a014
1097 110. Springer, A.M., McRoy, C.P., 1993. The paradox of pelagic food webs in the northern
1098 Bering Sea. III. Patterns of primary production. Cont. Shelf Res. 13, 575-599. Doi:
1099 10.1016/0278-4343(93)90095-F
1100 111. Springer, A.M., McRoy, C.P., Flint, M.V., 1996. The Bering Sea Green Belt: shelf-edge
1101 processes and ecosystem production. Fisheries Oceanography 5, 205-223. Doi:
1102 10.1111/j.1365-2419.1996.tb00118.x
1103 112. Steele, M., Ermold, W., Zhang, J., 2008. Arctic Ocean surface warming trends over the
1104 past 100 years. Geophys. Res. Lett. 35, L02614. Doi: 10.1029/2007GL031651
1105 113. Sun, M.-Y., Clough, L.M., Carroll, M.L., Dai, J., Ambrose Jr, W.G., Lopez, G.R., 2009.
1106 Different responses of two common Arctic macrobenthic species (*Macoma balthica* and
1107 *Monoporeia affinis*) to phytoplankton and ice algae: Will climate change impacts be species
1108 specific? J. Exp. Mar. Biol. Ecol. 376, 110–121. Doi: 10.1016/j.jembe.2009.06.018

114. R Development Core Team, 2018. R: A Language and Environment for Statistical Computing. R Foundation for Statistical Computing, Vienna.

115. Stock, B.C., Semmens, B.X., 2016. MixSIAR GUI User Manual. Version 3.1. https://github.com/brianstock/MixSIAR/. doi:10.5281/zenodo.47719.

116. Tabachnick, B.G., Fidell, L.S., 2013. Using Multivariate Statistics, 6th Edition. MyPsychLab Series.

117. Timmermans, M.L., Proshutinsky, A., 2015. Sea Surface Temperature. [in: Arctic Report Card 2015]. http://www.arctic.noaa.gov/Report-Card.

118. Timmermans, M.-L., Toole, J., Krishfield, R., 2018. Warming of the interior Arctic Ocean linked to sea ice losses at the basin margins. Sci. Adv. 4, eaat6773. Doi: 10.1126/sciadv.aat6773

119. Tu, K.L., Blanchard, A.L., Iken K., Horstmann-Dehn, L., 2015. Small-scale spatial variability in benthic food webs in the northeastern Chukchi Sea. Mar. Ecol. Progr. Ser. 528, 19-37. Doi: 10.3354/meps11216

120. Vokhshoori, N.L., Larsen, T., McCarthy, M.D., 2014. Reconstructing $\delta^{13}C$ isoscapes of phytoplankton production in a coastal upwelling system with amino acid isotope values of littoral mussels. Mar. Ecol. Progr. Ser. 504, 59-72. Doi: 10.3354/meps10746

121. Walsh, J.J., McRoy, C.P., Coachman, L.K., Goering, J.J., Nihoul, J.J., Whitledge, T.E., Blackbum, T.H., Parker, P.L., Wirick, C.D., Shuert, P.G., Grebmeier, J.M., Springer, A.M., Tripp, R.D., Hansell, D.A., Djenidi, S., Deleersnijder, E., Henriksen, K., Lund, B.A., Andersen, P., Muller-Karger, F.E., Dean, K., 1989. Carbon and nitrogen cycling within the Bering/Chukchi Seas: source regions of organic matter affecting AOU demands of the Arctic ocean. Progr. Oceanogr. 22, 279-361. Doi: 10.1016/0079-6611(89)90006-2

1132 122. Walsh, J.E., Fetterer, F., Stewart, J.S., Chapman, W.L., 2016. A database for depicting
1133 Arctic sea ice variations back to 1850. Geogr. Rev. 107, 89-107. Doi: 10.1111/j.1931-
1134 0846.2016.12195.x
1135 123. Weingartner, T.J., Aagaard, K., Woodgate, R., Danielson, S., Sasaki, Y., Cavalieri, D.,
1136 2005. Circulation on the north central Chukchi Sea shelf. Deep Sea Res. II 52, 3150-3174.
1137 Doi: 10.1016/j.dsr2.2005.10.015
1138 124. Whiteman, J.P., Elliott Smith, E.A., Besser, A.C., Newsome, S.D., 2019. A Guide to
1139 using compound-specific stable isotope analysis to study the fates of molecules in organisms
1140 and ecosystems. Diversity 11, 8. Doi: 10.3390/d11010008
1141 125. Woodgate, R.A. 2018. Increases in the Pacific inflow to the Arctic from 1990 to 2015,
1142 and insights into seasonal trends and driving mechanisms from year-round Bering Strait
1143 mooring data. Progress in Oceanogr. 160, 124–154. Doi: 10.1016/j.pocean.2017.12.007
1144 126. Woodgate, R.A., Aagaard, K., Weingartner, T.J., 2005a. Monthly temperature, salinity,
1145 and transport variability of the Bering Strait throughflow. Geophys. Res. Lett. 32, L04601.
1146 Doi: 10.1029/2004GL021880
1147 127. Woodgate, R.A., Aagaard, K., Weingartner, T.J., 2005b. A year in the physical
1148 oceanography of the Chukchi Sea: Moored measurements from autumn 1990–1991. Deep Sea
1149 Res. II 52, 3116–3149. Doi: 10.1016/j.dsr2.2005.10.016
1150 128. Woodgate, R., Weingartner, T., Lindsay, R., 2010. The 2007 Bering Strait oceanic heat
1151 flux and anomalous Arctic sea-ice retreat. Geophys. Res. Lett. 37, L01602. Doi:
1152 10.1029/2009GL041621
1153 129. Woodgate, R., Weingartner, T., Lindsay, R., 2012. Observed increases in Bering Strait
1154 oceanic fluxes from the Pacific to the Arctic from 2001 to 2011 and their impacts on the
1155 Arctic Ocean water column. Geophys. Res. Lett. 39, L24603. Doi: 10.1029/2012GL054092

130. Yurkowski, D.J., Brown, T.A., Blanchfield, P.J., Ferguson, S.H., 2020. Atlantic walrus signal latitudinal differences in the long-term decline of sea ice-derived carbon to benthic fauna in the Canadian Arctic. Proc. R. Soc. B 287, 20202126. Doi: 10.1098/rspb.2020.2126

131. Ziegler, S.E., Fogel, M.L., 2003. Seasonal and diel relationships between the isotopic compositions of dissolved and particulate organic matter in freshwater ecosystems. Biogeochemistry 64, 25-52. Doi: 10.1023/A:1024989915550